

# Bethe-Salpeter Equation for Heavy Baryons $\omega_Q^{(*)}$ in the Diquark Picture

X.-H. Guo<sup>1,2</sup>, A.W. Thomas<sup>1</sup> and A.G. Williams<sup>1</sup>

<sup>1</sup> Department of Physics and Mathematical Physics,  
and Special Research Center for the Subatomic Structure of Matter,  
University of Adelaide, SA 5005, Australia

<sup>2</sup> Institute of High Energy Physics, Academia Sinica, Beijing 100039, China  
e-mail: xhguo@physics.adelaide.edu.au, athomas@physics.adelaide.edu.au,  
awilliam@physics.adelaide.edu.au

## Abstract

In the heavy quark limit, the heavy baryons  $\omega_Q^{(*)}$  ( $\omega$  stands for  $\Sigma$ ,  $\Xi$  or  $\Omega$  and  $Q = b$  or  $c$ ) are regarded as composed of a heavy quark and an axial vector, light diquark with good spin and isospin quantum numbers. Based on this diquark picture we establish the Bethe-Salpeter (B-S) equation for  $\omega_Q^{(*)}$  in the limit where the heavy quark has infinite mass,  $m_Q \rightarrow \infty$ . It is found that in this limit there are three components in the B-S wave function for  $\omega_Q^{(*)}$ . Assuming the kernel to consist of a scalar confinement term and a one-gluon-exchange term we derive three coupled integral equations for the three B-S scalar functions in the covariant instantaneous approximation. Numerical solutions for the three B-S scalar functions are presented, including a discussion of their dependence on the various input parameters. These solutions are applied to calculate the Isgur-Wise functions  $\xi(\omega)$  and  $\zeta(\omega)$  for the weak transitions  $\Omega_b^{(*)} \rightarrow \Omega_c^{(*)}$ . Using these we give predictions for the Cabibbo-allowed nonleptonic decay widths and up-down asymmetries for  $\Omega_b \rightarrow \Omega_c^{(*)}$  plus a pseudoscalar or vector meson.

**PACS Numbers:** 11.10.St, 12.39.Hg, 14.20.Mr, 14.20.Lq

## I. Introduction

The physics of heavy hadrons has been a subject of intense interest in recent years. One reason for this is that more and more experimental data are being accumulated. Another reason is the discovery of the new flavor and spin symmetry in QCD,  $SU(2)_f \times SU(2)_s$ , in the heavy quark limit and the establishment of heavy quark effective theory (HQET) [1]. However, in comparison with the heavy meson case, heavy baryons have been studied much less, both experimentally and theoretically.

On the other hand, the experimental situation with heavy baryons has been improving recently, with more measurements becoming available. For instance, OPAL has measured some physical quantities for  $\Lambda_b$ , such as its lifetime and the production branching ratio for the inclusive semileptonic decay  $\Lambda_b \rightarrow \Lambda l^- \bar{\nu} X$  [2]. Furthermore, measurements of the nonleptonic decay of  $\Lambda_b$  have also been made, through the well-known process  $\Lambda_b \rightarrow \Lambda J/\psi$ . The discrepancy between the measurements made by UA1 [3] and those by CDF [4] and LEP [5] appears to have been settled by the new measurement from CDF [6]. However, compared with D and B mesons, the data for heavy baryons are still very limited. Besides  $\Lambda_b$ , there has been few data on other bottom baryons [7], although we expect more data to appear in the near future. Clearly the time is right for serious theoretical studies of heavy baryon properties to begin.

Theoretically, the HQET can simplify the physical processes involving heavy quarks, since with the aid of the HQET the number of independent form factors is reduced. For instance, in leading order of the  $1/m_Q$  expansion only one form factor (the Isgur-Wise function) remains for the  $\Lambda_b \rightarrow \Lambda_c$  transition, while for  $\omega_b^{(*)} \rightarrow \omega_c^{(*)}$  (we follow the notations of Ref.[8],  $\omega$  could be  $\Xi$ ,  $\Sigma$  or  $\Omega$  and  $Q = b$  or  $c$ ) there are two independent Isgur-Wise functions. (Note that  $\omega_Q^{(*)}$  is a notation implying either  $\omega_Q$  or  $\omega_Q^*$ .) The behaviour of these functions depends on the nonperturbative effects

of QCD which control the dynamics inside a heavy hadron. Hence some nonperturbative QCD model has to be adopted from which these Isgur-Wise functions can be obtained. In previous work [9], we established the B-S equation for  $\Lambda_Q$ , which is assumed to be composed of a heavy quark,  $Q$ , and a scalar diquark. Some theoretical predictions for  $\Lambda_b \rightarrow \Lambda_c$  were also obtained. It is the purpose of the present paper to generalize such an approach to the heavy baryons,  $\omega_Q^{(*)}$ , and consequently give some phenomenological predictions for the weak decays of such baryons.

When the quark mass is very heavy compared with the QCD scale,  $\Lambda_{\text{QCD}}$ , the light degrees of freedom in a heavy baryon  $\Lambda_Q$  ( $Q = b$  or  $c$ ) become blind to the flavor and spin quantum numbers of the heavy quark because of the  $SU(2)_f \times SU(2)_s$  symmetry. Therefore, the light degrees of freedom have good quantum numbers, including angular momentum and isospin. These quantum numbers can be used to classify heavy baryons. For example, the light degrees of freedom of  $\Lambda_Q$  have zero angular momentum and isospin. For  $\Sigma_Q^{(*)}$ , the angular momentum and parity  $J^P$  of the light degrees of freedom are  $1^+$ , and the isospin is also 1 in order to guarantee that the total wave function of the hadron is antisymmetric. Hence it is natural to consider the heavy baryon to be composed of a heavy quark and a light diquark. This is our underlying assumption.

Based on the picture of the composition of the heavy baryon which we have just presented, the three body system is simplified to a two body system. We establish the B-S equation for the heavy baryons,  $\omega_Q^{(*)}$ , in this picture. The heavy quark symmetry can be used to simplify the form of the B-S wave function greatly. It can be shown that in the limit  $m_Q \rightarrow \infty$  there are three components in the B-S wave function, and hence we have three corresponding scalar functions. We solve the B-S equation numerically by assuming that the kernel contains a scalar confinement term and a one-gluon-exchange term. The explicit dependence of the B-S wave function on the parameters of the model will be discussed. Furthermore, we calculate the Isgur-

Wise functions in terms of the B-S wave functions and give theoretical predictions for the Cabbibo-allowed two body nonleptonic decays  $\Omega_b \rightarrow \Omega_c^{(*)}$  plus a pseudoscalar or vector meson.

The light degrees of freedom of  $\omega_Q^{(*)}$  belong to a 6 representation of flavor SU(3). Taking  $Q = b$  as an example,  $\omega_b^{(*)}$  includes  $\Sigma_b^{(*)+,0,-}$ ,  $\Xi_b^{(*)0,-}$  and  $\Omega_b^{(*)-}$ . The total spin of  $\omega_Q$  and  $\omega_Q^*$  are  $\frac{1}{2}$  and  $\frac{3}{2}$  respectively. There is no strange quark in  $\Sigma_Q^{(*)}$  while there is one strange quark in  $\Xi_Q^{(*)}$  and two in  $\Omega_Q^{(*)}$  respectively.

The remainder of this paper is organized as follows. In Section II we establish the B-S equation for the heavy quark and axial vector light diquark system and discuss the form of the kernel. In Section III we derive explicitly the coupled integral equations for the B-S scalar wave functions. In Section IV we discuss the normalization condition of the B-S wave function by exploiting the normalization of the Isgur-Wise function at the zero recoil point. The numerical solutions of the B-S equation and their dependence on the parameters in our model are presented in Section V. In Section VI we calculate the Isgur-Wise functions and give predictions for the decay widths and up-down asymmetry parameters for  $\Omega_b \rightarrow \Omega_c^{(*)}$  plus a pseudoscalar or vector meson. Finally, Section VI contains a summary and discussions.

## II. The B-S equation for $\omega_Q^{(*)}$

As discussed in Section I,  $\omega_Q^{(*)}$  is regarded as a bound state of a heavy quark,  $\psi_Q$ , and a light axial vector diquark  $A_\mu$ . In the following,  $u_Q$  denotes the Dirac spinor of  $\psi_Q$  and  $\eta_\mu$  represents the polarization vector of  $A_\mu$ . Then  $B_\mu \equiv u_Q \eta_\mu$  can be decomposed into spin- $\frac{1}{2}$  and spin- $\frac{3}{2}$  states [10, 11] which represent  $\omega_Q$  and  $\omega_Q^*$  respectively. These two states are degenerate in the heavy quark limit. Using the notation of Refs. [11, 12] this doublet is described by  $B_\mu^m(v)$ , where  $m = 1, 2$  correspond to  $\omega_Q$  and  $\omega_Q^*$  respectively,  $v_\mu$  is the velocity of the heavy baryon and

$B_\mu = B_\mu^1 + B_\mu^2$  [10]. Explicitly, we can write

$$\begin{aligned} B_\mu^1(v) &= \frac{1}{\sqrt{3}}(\gamma_\mu + v_\mu)\gamma_5 u(v), \\ B_\mu^2(v) &= u_\mu(v), \end{aligned} \quad (1)$$

where  $u(v)$  is the Dirac spinor and  $u_\mu(v)$  is the Rarita-Schwinger vector spinor.

$B_\mu^m(v)$  satisfies the following conditions:

$$\not{v}B_\mu^m(v) = B_\mu^m(v), \quad v^\mu B_\mu^m(v) = 0, \quad \gamma^\mu B_\mu^2(v) = 0. \quad (2)$$

The above constraints for  $m = 1$  can be seen from  $\not{v}u(v) = u(v)$  while for  $m = 2$ , they are the properties of a spin- $\frac{3}{2}$ , Rarita-Schwinger vector spinor.

Under a Lorentz transformation  $\Lambda$ [10]

$$B_\mu \rightarrow \Lambda_\mu^\nu D(\Lambda) B_\nu, \quad (3)$$

where  $D(\Lambda)$  is the spinorial representation of  $\Lambda$ . Under the heavy quark spin transformation[8]

$$B_\mu \rightarrow -\gamma_5 \not{e} B_\mu, \quad (4)$$

where  $e = e_1, e_2, e_3$  are three mutually orthogonal four-dimensional unit vectors which are also orthogonal to  $v$ , (i.e.,  $e_i \cdot v = 0$ ), and  $e_i^2 = -1$  ( $i = 1, 2, 3$ ). The three unit vectors are associated with the heavy quark spin operators which are generators of the  $SU(2)_s$  symmetry.

Since  $\omega_Q^{(*)}$  is composed of  $\psi_Q$  and  $A_\mu$ , we can define the B-S wave function of  $\omega_Q^{(*)}$  by

$$\chi_\mu(x_1, x_2, P) = \langle 0 | T \psi_Q(x_1) A_\mu(x_2) | \omega_Q^{(*)}(P) \rangle, \quad (5)$$

where  $P = m_{\omega_Q^{(*)}} v$  is the total momentum of  $\omega_Q^{(*)}$  and  $v$  is its velocity. Let  $m_Q$  and  $m_D$  be the masses of the heavy quark and the light diquark in the baryon. Let us define  $\lambda_1 \equiv \frac{m_Q}{m_Q + m_D}$  and  $\lambda_2 \equiv \frac{m_D}{m_Q + m_D}$  and let  $p$  be the relative momentum of the

two constituents. The B-S wave function in momentum space is defined as

$$\chi_\mu^m(x_1, x_2, P) = e^{iP \cdot X} \int \frac{d^4 p}{(2\pi)^4} e^{ip \cdot x} \chi_{P\mu}^m(p), \quad (6)$$

where  $X \equiv \lambda_1 x_1 + \lambda_2 x_2$  is the coordinate of the center of mass and  $x \equiv x_1 - x_2$ . The momentum of the heavy quark is  $p_1 = \lambda_1 P + p$  and that of the diquark is  $p_2 = -\lambda_2 P + p$ .

It can be shown that  $\chi_{Pm}^\mu(p)$  satisfies the following B-S equation[13]

$$\chi_{Pm}^\mu(p) = S_F(\lambda_1 P + p) \int \frac{d^4 q}{(2\pi)^4} G_{\rho\nu}(P, p, q) \chi_{Pm}^\nu(q) S_D^{\mu\rho}(-\lambda_2 P + p), \quad (7)$$

where  $G_{\rho\nu}(P, p, q)$  is the kernel, which is defined as the sum of all the two particle irreducible diagrams with respect to the heavy quark and the light diquark. For convenience, in the following we use the variables

$$p_l \equiv v \cdot p - \lambda_2 m_{\omega_Q^{(*)}}, \quad p_t \equiv p - (v \cdot p)v. \quad (8)$$

Then in the leading order of the  $1/m_Q$  expansion we have

$$S_F(\lambda_1 P + p) = \frac{i(1 + \not{p})}{2(p_l + E_0 + m_D + i\epsilon)}, \quad (9)$$

where  $E_0$  is the binding energy. From Eqs.(7) and (9) it follows that  $\chi_{Pm}^\mu(p)$  satisfies the following equation

$$\not{p} \chi_{Pm}^\mu(p) = \chi_{Pm}^\mu(p). \quad (10)$$

The propagator of the light axial vector diquark has the form

$$S_{D\mu\nu}(p_2) = -i \frac{g_{\mu\nu} - p_{2\mu} p_{2\nu} / m_D^2}{p_l^2 - m_D^2 + i\epsilon}. \quad (11)$$

In the limit  $m_Q \rightarrow \infty$  we have  $p_2 = -m_D v + p$  and hence we have

$$S_{D\mu\nu}(p_2) = -i \frac{g_{\mu\nu} - v_\mu v_\nu - p_\mu p_\nu / m_D^2 + (v_\mu p_\nu + v_\nu p_\mu) / m_D}{p_l^2 - W_p^2 + i\epsilon}, \quad (12)$$

where  $W_p \equiv \sqrt{p_t^2 + m_D^2}$ . The corrections to Eqs.(9) and (12) are from  $O(1/m_Q)$  terms.

Now we discuss the form of the B-S wave function  $\chi_{Pm}^\mu(p)$ . In the heavy quark limit, due to the  $SU(2)_s \times SU(2)_f$  symmetry, the internal dynamics of the heavy baryon,  $\omega_Q^{(*)}$ , is determined by the light degrees of freedom and the flavor and spin direction of the heavy quark,  $Q$ , is irrelevant. Consequently we have[10, 12]

$$\chi_P^\mu(p) = u_Q(v)\eta_\nu\zeta^{\mu\nu}(v,p), \quad (13)$$

and

$$\langle 0|A_\mu|\text{light}, 1^+ \rangle = \eta_\nu\zeta^{\mu\nu}(v,p). \quad (14)$$

Since  $v \cdot \eta = 0$ [10], the tensor  $\zeta^{\mu\nu}(v,p)$  can be expanded as

$$\zeta^{\mu\nu}(v,p) = A_1 g^{\mu\nu} + A_2 v^\mu p^\nu + A_3 p^\mu p^\nu, \quad (15)$$

where  $A_i (i = 1, 2, 3)$  are Lorentz scalar functions. After expressing  $u_Q\eta_\mu$  in Eq.(13) in terms of  $B_\mu^m(v)$  ( $m = 1, 2$ ), we have the following form for the B-S wave function

$$\chi_{Pm}^\mu = A_1 B_m^\mu(v) + A_2 v^\mu p_\nu B_m^\nu(v) + A_3 p^\mu p_\nu B_m^\nu(v). \quad (16)$$

Therefore, we have three components in the B-S wave function,  $\chi_{Pm}^\mu(p)$ , and they correspond to three scalar B-S functions  $A_i (i = 1, 2, 3)$ . This is consistent with our diquark picture for  $\omega_Q^{(*)}$ . In the heavy quark limit, the dynamics inside the heavy baryon is controlled by the configuration of the light degrees of freedom. Since the light diquark is a  $1^+$  object, it has three different configurations. Consequently there are three components in the B-S wave function which describe the dynamics in the heavy baryon  $\omega_Q^{(*)}$ .

In fact, we can derive the form of  $\chi_{Pm}^\mu(p)$  in another way. We may first write out all the possible terms which have the same behaviour as  $\chi_{Pm}^\mu(p)$  under Lorentz transformations. Then by applying the condition Eq.(10) and ensuring the proper

behaviour under the heavy quark spin transformation, Eq.(4), we obtain the same result as given in Eq.(16).

Considering  $p^\mu = v \cdot p v^\mu + p_t^\mu$ , and using the constraint  $v^\mu B_\mu^m(v) = 0$ , it will be convenient to define

$$A = A_1, \quad C = A_2 + v \cdot p A_3, \quad D = A_3,$$

which results in the following expression for the B-S wave function:

$$\chi_{Pm}^\mu = AB_m^\mu(v) + Cv^\mu p_{t\nu} B_m^\nu(v) + Dp_t^\mu p_{t\nu} B_m^\nu(v). \quad (17)$$

$A, C$  and  $D$  in Eq.(17) are functions of  $p_l$  and  $p_t^2$ . Their behaviour is controlled by nonperturbative QCD. Our aim is to obtain explicit forms for them with some QCD-motivated model for the form of the B-S kernel.

Motivated by the success of the potential model[14], scalar confinement and one-gluon-exchange terms were used in the kernel when studying  $\Lambda_Q$  in Ref.[9]. This form was also used in the heavy meson case in Ref.[15]. In the present work we will also adopt this form of the kernel

$$iG^{\rho\nu} = g^{\rho\nu} I \otimes IV_1 + v_\mu \otimes \Gamma^{\mu\rho\nu} V_2, \quad (18)$$

where  $\Gamma^{\mu\rho\nu}$  is the vertex of a gluon with two axial vector diquarks. This vertex should reflect the internal structure of the diquark. In this work, we use the model proposed in Ref.[16] where this vertex has the following form (see Fig. 1)

$$-i\frac{\lambda^a}{2}g_s\Gamma^{\mu\rho\nu}F_V(Q^2), \quad (19)$$

with

$$\Gamma^{\mu\rho\nu} = (p_2 + p_2')^\mu g^{\nu\rho} - (p_2^\nu g^{\mu\rho} + p_2'^\rho g^{\mu\nu}).$$

In Eq.(19)  $g_s$  is the strong interaction coupling constant and  $F_V(Q^2)$  is introduced to describe the internal structure of the axial vector diquark. The form factor,  $F_V(Q^2)$ ,



depends on nonperturbative QCD interactions and will be determined phenomenologically, by comparison with experiment.

As discussed in Ref.[9], when we consider the vertex of two heavy quarks with a gluon, the momenta of the two heavy quarks are  $p_1 = \lambda_1 m_{\Lambda_Q} v + p$  and  $p'_1 = \lambda_1 m_{\Lambda_Q} v + q$  respectively, where  $p$  and  $q$  are relative momenta and of the order  $\Lambda_{QCD}$ . In the heavy quark limit the heavy quark is almost on-shell and moves with constant velocity. It can be shown that  $p_l = q_l$  at this vertex when the heavy quark is exactly on-shell. This is the so-called covariant instantaneous approximation [9, 15]. With this approximation,  $V_1$  and  $V_2$  in  $G^{\rho\nu}(P, p, q)$  are replaced by

$$\tilde{V}_i \equiv V_i|_{p_l=q_l} (i = 1, 2). \quad (20)$$

### III. Coupled integral equations for three B-S scalar wave functions

In this section we will derive explicitly three coupled integral equations for the B-S scalar wave functions. Substituting Eqs.(9) and (12) into Eq.(7) and considering the form of the kernel in Eq.(18) and the property in Eq.(10), we obtain the following form for the B-S equation

$$\chi_{Pm}^\mu(p) = \frac{-i}{(p_l + E_0 + m_D + i\epsilon)(p_l^2 - W_p^2 + i\epsilon)} M_m^\mu, \quad (21)$$

where

$$M_{m\mu} \equiv i \left[ g_{\mu\rho} - v_\mu v_\rho + \frac{(v_\mu p_\rho + p_\mu v_\rho)}{m_D} - \frac{p_\mu p_\rho}{m_D^2} \right] \int \frac{d^4 q}{(2\pi)^4} [G^{\rho\nu}(P, p, q) \chi_{Pm\nu}(q)]|_{p_l=q_l}, \quad (22)$$

and we have made explicit use of the covariant instantaneous approximation.

Substituting Eqs.(17), (18) and (19) into Eq.(22) and again using the covariant instantaneous approximation we have

$$M_m^\mu = B_m^\mu(v) \int \frac{d^4 q}{(2\pi)^4} A(\tilde{V}_1 + 2p_l \tilde{V}_2) + \frac{1}{m_D} v^\mu \int \frac{d^4 q}{(2\pi)^4} \{p_t \cdot B_m(v) A(\tilde{V}_1 + 2p_l \tilde{V}_2)$$

$$\begin{aligned}
& +(p_l + m_D)[-Ap_t \cdot B_m(v)\tilde{V}_2 + q_t \cdot B_m(v)(C\tilde{V}_1 - Dp_t \cdot q_t\tilde{V}_2)] \\
& + p_t \cdot q_t q_t \cdot B_m(v)[-C\tilde{V}_2 + D(\tilde{V}_1 + 2p_l\tilde{V}_2)]\} - \frac{1}{m_D^2} p^\mu \int \frac{d^4 q}{(2\pi)^4} \\
& \{p_t \cdot B_m(v)A(\tilde{V}_1 + 2p_l\tilde{V}_2) + p_l[-Ap_t \cdot B_m(v)\tilde{V}_2 \\
& + q_t \cdot B_m(v)(C\tilde{V}_1 - Dp_t \cdot q_t\tilde{V}_2)] + p_t \cdot q_t q_t \cdot B_m(v)[-C\tilde{V}_2 + D(\tilde{V}_1 + 2p_l\tilde{V}_2)]\} \\
& + \int \frac{d^4 q}{(2\pi)^4} q_t^\mu q_t \cdot B_m(v)[-C\tilde{V}_2 + D(\tilde{V}_1 + 2p_l\tilde{V}_2)]. \tag{23}
\end{aligned}$$

We notice that in Eq.(23) there are terms of the form  $\int \frac{d^4 q}{(2\pi)^4} q_t^\mu f$  and  $\int \frac{d^4 q}{(2\pi)^4} q_t^\mu q_t^\nu f$ , where  $f$  is some function of  $p^2, q^2$ , and  $p \cdot q$ . On the grounds of Lorentz invariance, in general we have

$$\int \frac{d^4 q}{(2\pi)^4} q_t^\mu f = f_1 v^\mu + f_2 p_t^\mu, \tag{24}$$

and

$$\int \frac{d^4 q}{(2\pi)^4} q_t^\mu q_t^\nu f = g_1 g^{\mu\nu} + g_2 v^\mu v^\nu + g_3 v^\mu p_t^\nu + g_4 v^\nu p_t^\mu + g_5 p_t^\mu p_t^\nu. \tag{25}$$

From Eq.(24) only the  $f_2$  term can contribute, while from Eq.(25) only the  $g_1, g_3$  and  $g_5$  terms can contribute, since  $v_\nu B_m^\nu(v) = 0$ . It can be easily shown that

$$\begin{aligned}
f_2 &= \int \frac{d^4 q}{(2\pi)^4} \frac{p_t \cdot q_t}{p_t^2} f, \\
g_1 &= \int \frac{d^4 q}{(2\pi)^4} \frac{(p_t \cdot q_t)^2 - p_t^2 q_t^2}{2p_t^2} f, \\
g_3 &= 0, \\
g_5 &= \int \frac{d^4 q}{(2\pi)^4} \frac{3(p_t \cdot q_t)^2 - p_t^2 q_t^2}{2p_t^4} f. \tag{26}
\end{aligned}$$

With the aid of Eqs.(24), (25) and (26) we can express  $M_m^\mu$  in Eq.(23) in terms of  $B_m^\mu(v)$ ,  $v^\mu p_{t\nu} B_m^\nu(v)$  and  $p_t^\mu p_{t\nu} B_m^\nu(v)$ . Let us define

$$\tilde{A}(p_t^2) = \int \frac{dq_l}{2\pi} A(p_l, p_t^2), \quad \tilde{C}(p_t^2) = \int \frac{dq_l}{2\pi} C(p_l, p_t^2), \quad \tilde{D}(p_t^2) = \int \frac{dq_l}{2\pi} D(p_l, p_t^2), \tag{27}$$

where  $\tilde{A}$ ,  $\tilde{C}$  and  $\tilde{D}$  are functions of  $p_t^2$  only. Then one obtains the expression

$$M_m^\mu = B_m^\mu(v) \int \frac{d^3 q_t}{(2\pi)^3} \left\{ \tilde{A}(\tilde{V}_1 + 2p_l\tilde{V}_2) - \tilde{C} \frac{(p_t \cdot q_t)^2 - p_t^2 q_t^2}{2p_t^2} \tilde{V}_2 \right.$$

$$\begin{aligned}
& + \tilde{D} \frac{(p_t \cdot q_t)^2 - p_t^2 q_t^2}{2p_t^2} (\tilde{V}_1 + 2p_l \tilde{V}_2) \Big\} \\
& + \frac{1}{m_D^2} v^\mu p_t \cdot B_m(v) \int \frac{d^3 q_t}{(2\pi)^3} \Big\{ -\tilde{A} [p_l \tilde{V}_1 + (p_l^2 + m_D^2) \tilde{V}_2] \\
& - \tilde{C} \left[ (p_l^2 - m_D^2) \frac{p_t \cdot q_t}{p_t^2} \tilde{V}_1 + p_l \frac{(p_t \cdot q_t)^2}{p_t^2} \tilde{V}_2 \right] \\
& + \tilde{D} \frac{(p_t \cdot q_t)^2}{p_t^2} [p_l \tilde{V}_1 + (p_l^2 + m_D^2) \tilde{V}_2] \Big\} \\
& - \frac{1}{m_D^2} p_t^\mu p_t \cdot B_m(v) \int \frac{d^3 q_t}{(2\pi)^3} \Big\{ \tilde{A} (\tilde{V}_1 + p_l \tilde{V}_2) \\
& + \tilde{C} \left[ p_l \frac{p_t \cdot q_t}{p_t^2} \tilde{V}_1 + \frac{m_D^2 (3(p_t \cdot q_t)^2 - p_t^2 q_t^2) + 2p_t^2 (p_t \cdot q_t)^2}{2p_t^4} \tilde{V}_2 \right] \\
& + \tilde{D} \left[ -\frac{m_D^2 (3(p_t \cdot q_t)^2 - p_t^2 q_t^2) + 2p_t^2 (p_t \cdot q_t)^2}{2p_t^4} (\tilde{V}_1 + 2p_l \tilde{V}_2) \right. \\
& \left. + p_l \frac{(p_t \cdot q_t)^2}{p_t^2} \tilde{V}_2 \right] \Big\}. \tag{28}
\end{aligned}$$

In Eq.(21) there are poles in  $p_l$  at  $W_p - i\epsilon, -W_p + i\epsilon$  and  $-E_0 - m_D - i\epsilon$ . By choosing the appropriate contour, we integrate over  $p_l$  on both sides of Eq.(21) and obtain the following, three coupled integral equations for  $\tilde{A}, \tilde{C}$  and  $\tilde{D}$

$$\begin{aligned}
\tilde{A}(p_t^2) = & \frac{-1}{2W_p(E_0 + m_D - W_p)} \int \frac{d^3 q_t}{(2\pi)^3} \Big\{ \tilde{A}(q_t^2) (\tilde{V}_1 - 2W_p \tilde{V}_2) \\
& - \tilde{C}(q_t^2) \frac{(p_t \cdot q_t)^2 - p_t^2 q_t^2}{2p_t^2} \tilde{V}_2 + \tilde{D}(q_t^2) \frac{(p_t \cdot q_t)^2 - p_t^2 q_t^2}{2p_t^2} (\tilde{V}_1 - 2W_p \tilde{V}_2) \Big\}, \tag{29}
\end{aligned}$$

$$\begin{aligned}
\tilde{C}(p_t^2) = & \frac{-1}{2m_D^2 W_p (E_0 + m_D - W_p)} \int \frac{d^3 q_t}{(2\pi)^3} \Big\{ \tilde{A}(q_t^2) [W_p \tilde{V}_1 \\
& - ((E_0 + m_D) W_p + m_D^2) \tilde{V}_2] \\
& + \tilde{C}(q_t^2) \left[ -\frac{p_t \cdot q_t}{p_t^2} ((E_0 + m_D) W_p - m_D^2) \tilde{V}_1 + W_p \frac{(p_t \cdot q_t)^2}{p_t^2} \tilde{V}_2 \right] \\
& + \tilde{D}(q_t^2) \frac{(p_t \cdot q_t)^2}{p_t^2} [-W_p \tilde{V}_1 + ((E_0 + m_D) W_p + m_D^2) \tilde{V}_2] \Big\}, \tag{30}
\end{aligned}$$

$$\begin{aligned}
\tilde{D}(p_t^2) = & \frac{1}{2m_D^2 W_p (E_0 + m_D - W_p)} \int \frac{d^3 q_t}{(2\pi)^3} \Big\{ \tilde{A}(q_t^2) (\tilde{V}_1 - W_p \tilde{V}_2) \\
& + \tilde{C}(q_t^2) \left[ -\frac{p_t \cdot q_t}{p_t^2} W_p \tilde{V}_1 + \frac{m_D^2 (3(p_t \cdot q_t)^2 - p_t^2 q_t^2) + 2p_t^2 (p_t \cdot q_t)^2}{2p_t^4} \tilde{V}_2 \right]
\end{aligned}$$

$$\begin{aligned}
& -\tilde{D}(q_t^2) \left[ \frac{m_D^2(3(p_t \cdot q_t)^2 - p_t^2 q_t^2) + 2p_t^2(p_t \cdot q_t)^2}{2p_t^4} (\tilde{V}_1 - 2W_p \tilde{V}_2) \right. \\
& \left. + \frac{(p_t \cdot q_t)^2}{p_t^2} W_p \tilde{V}_2 \right] \Bigg\}. \tag{31}
\end{aligned}$$

If one knows the form for the kernel,  $\tilde{V}_1$  and  $\tilde{V}_2$ , then  $A(p_t^2), \tilde{C}(p_t^2)$  and  $\tilde{D}(p_t^2)$  can be obtained from Eqs.(29), (30) and (31). Consequently from Eqs. (17), (21) and (28) we find the following expressions for  $A(p_l, p_t^2)$ ,  $C(p_l, p_t^2)$  and  $D(p_l, p_t^2)$ :

$$\begin{aligned}
A(p_l, p_t^2) = & \frac{-i}{(p_l + E_0 + m_D + i\epsilon)(p_l^2 - W_p^2 + i\epsilon)} \int \frac{d^3 q_t}{(2\pi)^3} \left\{ \tilde{A}(q_t^2)(\tilde{V}_1 + 2p_l \tilde{V}_2) \right. \\
& \left. - \tilde{C}(q_t^2) \frac{(p_t \cdot q_t)^2 - p_t^2 q_t^2}{2p_t^2} \tilde{V}_2 + \tilde{D}(q_t^2) \frac{(p_t \cdot q_t)^2 - p_t^2 q_t^2}{2p_t^2} (\tilde{V}_1 + 2p_l \tilde{V}_2) \right\}, \tag{32}
\end{aligned}$$

$$\begin{aligned}
C(p_l, p_t^2) = & \frac{-i}{m_D^2(p_l + E_0 + m_D + i\epsilon)(p_l^2 - W_p^2 + i\epsilon)} \int \frac{d^3 q_t}{(2\pi)^3} \left\{ -\tilde{A}(q_t^2)[p_l \tilde{V}_1 \right. \\
& + (p_l^2 + m_D^2) \tilde{V}_2] - \tilde{C}(q_t^2) \left[ (p_l^2 - m_D^2) \frac{p_t \cdot q_t}{p_t^2} \tilde{V}_1 + p_l \frac{(p_t \cdot q_t)^2}{p_t^2} \tilde{V}_2 \right] \\
& \left. + \tilde{D}(q_t^2) \frac{(p_t \cdot q_t)^2}{p_t^2} [p_l \tilde{V}_1 + (p_l^2 + m_D^2) \tilde{V}_2] \right\}, \tag{33}
\end{aligned}$$

$$\begin{aligned}
D(p_l, p_t^2) = & \frac{i}{m_D^2(p_l + E_0 + m_D + i\epsilon)(p_l^2 - W_p^2 + i\epsilon)} \int \frac{d^3 q_t}{(2\pi)^3} \left\{ \tilde{A}(q_t^2)(\tilde{V}_1 + p_l \tilde{V}_2) \right. \\
& + \tilde{C}(q_t^2) \left[ \frac{p_t \cdot q_t}{p_t^2} p_l \tilde{V}_1 + \frac{m_D^2(3(p_t \cdot q_t)^2 - p_t^2 q_t^2) + 2p_t^2(p_t \cdot q_t)^2}{2p_t^4} \tilde{V}_2 \right] \\
& + \tilde{D}(q_t^2) \left[ -\frac{m_D^2(3(p_t \cdot q_t)^2 - p_t^2 q_t^2) + 2p_t^2(p_t \cdot q_t)^2}{2p_t^4} (\tilde{V}_1 + 2p_l \tilde{V}_2) \right. \\
& \left. \left. + \frac{(p_t \cdot q_t)^2}{p_t^2} p_l \tilde{V}_2 \right] \right\}. \tag{34}
\end{aligned}$$

A model kernel, specified in terms of  $\tilde{V}_1$  and  $\tilde{V}_2$ , for the B-S equation in the scalar light diquark case was given in Ref.[9]. In the present axial vector diquark case, a model vertex for a gluon with two  $1^+$  diquarks is given in Eq.(19), where  $F_V(Q^2)$  describes the internal structure of the light diquark. Following Ref.[16] we take the form for  $F_V(Q^2)$  as

$$F_V(Q^2) = \frac{\alpha_s^{(\text{eff})} Q_1^2}{Q^2 + Q_1^2}, \tag{35}$$

where  $Q_1^2$  is a parameter which freezes  $F_V(Q^2)$  when  $Q^2$  is very small. In the high energy region the form factor is proportional to  $1/Q^2$ , which is consistent with perturbative QCD calculations [17]. By analyzing the electromagnetic form factor for the proton it was found that selecting  $Q_1^2 = 3.2\text{GeV}^2$  can lead to results consistent with the experimental data [16]. Note that in Eq.(35) we do not consider the difference between longitudinal and transverse polarization states. The reason is that we are considering the bound state with a binding energy of order  $\Lambda_{\text{QCD}}$ , so this difference should be small (see Ref.[16], where this difference is a factor  $\frac{Q_2^2}{Q^2+Q_2^2}$  with  $Q_2^2$  approximately  $15\text{GeV}^2$ , so this factor is close to 1 in our discussions).

Based on the above discussion, the kernel for the B-S equation in the baryon case is taken to have the following form

$$\begin{aligned}\tilde{V}_1 &= \frac{8\pi\kappa}{[(p_t - q_t)^2 + \mu^2]^2} - (2\pi)^3 \delta^3(p_t - q_t) \int \frac{d^3k}{(2\pi)^3} \frac{8\pi\kappa}{(k^2 + \mu^2)^2}, \\ \tilde{V}_2 &= -\frac{16\pi}{3} \frac{\alpha_s^{(\text{eff})2} Q_1^2}{[(p_t - q_t)^2 + \mu^2][(p_t - q_t)^2 + Q_1^2]},\end{aligned}\tag{36}$$

where  $\kappa$  and  $\alpha_s^{(\text{eff})}$  are coupling parameters related to scalar confinement and the one-gluon-exchange diagram respectively. The second term in Eq.(36) is the counter term which removes the infra-red divergence arising from the linear confinement in the integral equation. The parameter  $\mu$  is introduced to avoid the infra-red divergence in numerical calculations. The limit  $\mu \rightarrow 0$  is taken in the end. Besides  $Q_1^2$ , there are two parameters  $\kappa$ , and  $\alpha_s^{(\text{eff})}$ , in the kernel. However, they should be related to each other when we solve the coupled integral equations (29), (30) and (31). This will be discussed in detail in Section V.

Since we now have an explicit form for  $\tilde{V}_1$  and  $\tilde{V}_2$  in Eq.(36), we can reduce Eqs.(29), (30) and (31) to one dimensional integral equations. With the aid of the formulas given in Appendix A we obtain the following equations from Eqs.(29), (30) and (31).

$$\tilde{A}(p_t^2) = \frac{-1}{2W_p(E_0 + m_D - W_p)} \int \frac{q_t^2 dq_t}{4\pi^2} \{ [8\pi\kappa F_1(|p_t|, |q_t|) + \frac{32\pi\beta W_p}{3(Q_1^2 - \mu^2)}]$$

$$\begin{aligned}
& (F_2(|p_t|, |q_t|, \mu) - F_2(|p_t|, |q_t|, Q_1))\tilde{A}(q_t^2) - 8\pi\kappa F_1(|p_t|, |q_t|)\tilde{A}(p_t^2)\} \\
& - \frac{1}{2W_p(E_0 + m_D - W_p)} \int \frac{q_t^2 dq_t}{4\pi^2} \frac{8\pi\beta}{3(Q_1^2 - \mu^2)} \{q_t^2[-F_2(|p_t|, |q_t|, \mu) \\
& + F_2(|p_t|, |q_t|, Q_1)] - \frac{1}{p_t^2}[(F_4(|p_t|, |q_t|, \mu) - F_4(|p_t|, |q_t|, Q_1))]\}\tilde{C}(q_t^2) \\
& + \frac{1}{2W_p(E_0 + m_D - W_p)} \int \frac{q_t^2 dq_t}{4\pi^2} \{4\pi\kappa[q_t^2 F_1(|p_t|, |q_t|) - \frac{1}{p_t^2} F_5(|p_t|, |q_t|)] \\
& + \frac{16\pi\beta W_p}{3(Q_1^2 - \mu^2)}[q_t^2(F_2(|p_t|, |q_t|, \mu) - F_2(|p_t|, |q_t|, Q_1)) \\
& + \frac{1}{2p_t^2}(F_4(|p_t|, |q_t|, \mu) - F_4(|p_t|, |q_t|, Q_1))]\}\tilde{D}(q_t^2), \tag{37}
\end{aligned}$$

$$\begin{aligned}
\tilde{C}(p_t^2) = & \frac{-1}{2m_D^2 W_p(E_0 + m_D - W_p)} \int \frac{q_t^2 dq_t}{4\pi^2} \{[8\pi\kappa W_p F_1(|p_t|, |q_t|) + \frac{16\pi\beta}{3(Q_1^2 - \mu^2)} \\
& (F_2(|p_t|, |q_t|, \mu) - F_2(|p_t|, |q_t|, Q_1))((E_0 + m_D)W_p + m_D^2)]\tilde{A}(q_t^2) \\
& - 8\pi\kappa W_p F_1(|p_t|, |q_t|)\tilde{A}(p_t^2)\} - \frac{1}{2m_D^2 W_p(E_0 + m_D - W_p)} \int \frac{q_t^2 dq_t}{4\pi^2} \\
& \{[8\pi\kappa F_3(|p_t|, |q_t|)]\frac{m_D^2 - (E_0 + m_D)W_p}{p_t^2} \\
& + \frac{16\pi\beta}{3(Q_1^2 - \mu^2)}(F_4(|p_t|, |q_t|, \mu) - F_4(|p_t|, |q_t|, Q_1))\frac{W_p}{p_t^2}]\tilde{C}(q_t^2) \\
& - 8\pi\kappa F_1(|p_t|, |q_t|)[m_D^2 - (E_0 + m_D)W_p]\tilde{C}(p_t^2)\} \\
& + \frac{1}{2m_D^2 W_p(E_0 + m_D - W_p)} \int \frac{q_t^2 dq_t}{4\pi^2} \{[8\pi\kappa F_5(|p_t|, |q_t|)]\frac{W_p}{p_t^2} \\
& - \frac{16\pi\beta}{3(Q_1^2 - \mu^2)}(F_4(|p_t|, |q_t|, \mu) - F_4(|p_t|, |q_t|, Q_1)) \\
& \frac{(E_0 + m_D)W_p + m_D^2}{p_t^2}]\tilde{D}(q_t^2) - 8\pi\kappa p_t^2 W_p F_1(|p_t|, |q_t|)\tilde{D}(p_t^2)\}, \tag{38}
\end{aligned}$$

$$\begin{aligned}
\tilde{D}(p_t^2) = & \frac{1}{2m_D^2 W_p(E_0 + m_D - W_p)} \int \frac{q_t^2 dq_t}{4\pi^2} \{[8\pi\kappa F_1(|p_t|, |q_t|) + \frac{16\pi\beta W_p}{3(Q_1^2 - \mu^2)} \\
& (F_2(|p_t|, |q_t|, \mu) - F_2(|p_t|, |q_t|, Q_1))]\tilde{A}(q_t^2) - 8\pi\kappa F_1(|p_t|, |q_t|)\tilde{A}(p_t^2)\} \\
& + \frac{1}{2m_D^2 W_p(E_0 + m_D - W_p)} \int \frac{q_t^2 dq_t}{4\pi^2} \{[-8\pi\kappa F_3(|p_t|, |q_t|)]\frac{W_p}{p_t^2} \\
& + \frac{16\pi\beta}{3(Q_1^2 - \mu^2)}(F_4(|p_t|, |q_t|, \mu) - F_4(|p_t|, |q_t|, Q_1))\frac{2p_t^2 + 3m_D^2}{2p_t^4} \\
& + \frac{16\pi\beta}{3(Q_1^2 - \mu^2)}(F_2(|p_t|, |q_t|, \mu) - F_2(|p_t|, |q_t|, Q_1))\frac{q_t^2 m_D^2}{2p_t^2}]\tilde{C}(q_t^2) \\
& + 8\pi\kappa W_p F_1(|p_t|, |q_t|)\tilde{C}(p_t^2)\}
\end{aligned}$$

$$\begin{aligned}
& -\frac{1}{2m_D^2 W_p(E_0 + m_D - W_p)} \int \frac{q_t^2 dq_t}{4\pi^2} \{ [8\pi\kappa F_5(|p_t|, |q_t|) \frac{2p_t^2 + 3m_D^2}{2p_t^4} \\
& - 8\pi\kappa F_1(|p_t|, |q_t|) \frac{q_t^2 m_D^2}{2p_t^2} - \frac{16\pi\beta}{3(Q_1^2 - \mu^2)} \\
& (F_4(|p_t|, |q_t|, \mu) - F_4(|p_t|, |q_t|, Q_1)) \frac{W_p(p_t^2 + 3m_D^2)}{p_t^4} \\
& - \frac{16\pi\beta}{3(Q_1^2 - \mu^2)} (F_2(|p_t|, |q_t|, \mu) - F_2(|p_t|, |q_t|, Q_1)) \frac{W_p m_D^2 q_t^2}{p_t^2} ] \tilde{D}(q_t^2) \\
& - 8\pi\kappa(p_t^2 + m_D^2) F_1(|p_t|, |q_t|) \tilde{D}(p_t^2) \}, \tag{39}
\end{aligned}$$

where  $|p_t| = \sqrt{p_t^2}$ . The functions  $F_i (i = 1, \dots, 5)$ , appearing in Eqs.(37), (38) and (39), are defined in Appendix A. From these three coupled integral equations we can solve numerically for  $\tilde{A}(p_t^2)$ ,  $\tilde{C}(p_t^2)$  and  $\tilde{D}(p_t^2)$ . This will be done in Section V. In the next section, we will first discuss the normalization of the B-S wave function.

## IV. Normalization for the B-S wave function

It can be seen that the overall normalization of  $\tilde{A}(p_t^2)$ ,  $\tilde{C}(p_t^2)$  and  $\tilde{D}(p_t^2)$  cannot be determined from Eqs.(37), (38) and (39). With the help of heavy quark symmetry, the normalization constant can be obtained from the fact that the Isgur-Wise function is normalized to one at the zero-recoil point. In the limit  $m_Q \rightarrow \infty$  the weak transition matrix element induced by the current  $\bar{c}\Gamma b$  for  $\omega_b^{(*)} \rightarrow \omega_c^{(*)}$  has the following form from the HQET,

$$\langle \omega_c^{(*)}(v') | \bar{c}\Gamma b | \omega_b^{(*)}(v) \rangle = \bar{B}_{m'}^\nu(v') \Gamma B_m^\mu(v) (\xi(\omega) g_{\mu\nu} + \zeta(\omega) v_\nu v'_\mu), \tag{40}$$

where  $\omega = v \cdot v'$  is the velocity transfer,  $m, m'$  could be 1 or 2, and  $\Gamma$  is an arbitrary Dirac matrix. At the zero-recoil point,  $v = v'$ , only the  $\xi(\omega) g_{\mu\nu}$  term contributes and we must have

$$\xi(\omega = 1) = 1. \tag{41}$$

On the other hand, the transition matrix element for  $\omega_b^{(*)} \rightarrow \omega_c^{(*)}$  is related to

the B-S wave functions of  $\omega_b^{(*)}$  and  $\omega_c^{(*)}$  by the following equation

$$\langle \omega_c^{(*)}(v') | \bar{c} \Gamma b | \omega_b^{(*)}(v) \rangle = \int \frac{d^4 p}{(2\pi)^4} \bar{\chi}_{P'm'}^\mu(p') \Gamma \chi_{Pm}^\nu(p) S_{D\mu\nu}^{-1}(p_2), \quad (42)$$

where  $P$  ( $P'$ ) is the momentum of  $\omega_b^{(*)}$  ( $\omega_c^{(*)}$ ) and  $\bar{\chi}_{P'm'}^\mu(p')$  is the wave function of the final state  $\omega_c^{(*)}(v')$ , which satisfies the constraint

$$\bar{\chi}_{P'm'}^\mu(p') \not{p}' = \bar{\chi}_{P'm'}^\mu(p'). \quad (43)$$

At the zero-recoil point,  $p' = p$ , since the light diquark sees no change in the heavy quark part it does not change its relative momentum.

The scalar B-S functions of the final state B-S wave function obey the same B-S equation as (29), (30) and (31). Substituting Eq.(7) into Eq.(42) and using Eq.(40) we have

$$\xi(1) \bar{B}_{m'\mu}(v) \Gamma B_m^\mu(v) = \int \frac{d^4 p}{(2\pi)^4} \frac{i}{p_l + E_0 + m_D + i\epsilon} \bar{\chi}_{Pm'}^\mu(p) \Gamma \int \frac{d^4 q}{(2\pi)^4} G_{\mu\nu}(P, p, q) \chi_{Pm}^\nu(p). \quad (44)$$

Now we substitute the expression for the kernel Eq.(18) and Eq.(17) into Eq.(44). Using the same technique as used for Eqs.(24), (25) and (26), we find that there is only the structure  $\bar{B}_{m'}^\mu(v) \Gamma B_{m\mu}(v)$  on the right hand side of Eq.(44). Substituting the explicit expressions for  $\tilde{V}_1$  and  $\tilde{V}_2$  in Eq.(36), and using the integration formula in Appendix A, we arrive at the following expression for  $\xi(1)$  after some tedious calculations

$$\begin{aligned} \xi(1) = & \int \frac{p_t^2 dp_t}{4\pi^2} \frac{2}{E_0 + m_D - W_p} \left[ \tilde{A}(p_t^2) h_1(|p_t|) - \frac{1}{3} p_t^2 \tilde{C}(p_t^2) h_2(|p_t|) \right. \\ & \left. - \frac{1}{3} p_t^2 \tilde{D}(p_t^2) h_3(|p_t|) + \frac{1}{6m_D^2} p_t^2 h_2(|p_t|) h_4(|p_t|) \right], \end{aligned} \quad (45)$$

where  $h_i(|p_t|)$  ( $i = 1, 2, 3, 4$ ) are given by the following equations

$$\begin{aligned} h_1(|p_t|) = & \int \frac{q_t^2 dq_t}{4\pi^2} \{ 8\pi\kappa F_1(|p_t|, |q_t|) [\tilde{A}(q_t^2) - \frac{1}{3} q_t^2 \tilde{D}(q_t^2)] + \frac{16\pi\beta}{3(Q_1^2 - \mu^2)} \\ & [F_2(|p_t|, |q_t|, \mu) - F_2(|p_t|, |q_t|, Q_1)] [2W_p \tilde{A}(q_t^2) - \frac{1}{3} q_t^2 \tilde{C}(q_t^2) \\ & - \frac{2}{3} W_p q_t^2 \tilde{D}(q_t^2)] - 8\pi\kappa F_1(|p_t|, |q_t|) [\tilde{A}(p_t^2) - \frac{1}{3} p_t^2 \tilde{D}(p_t^2)] \}, \end{aligned} \quad (46)$$



$$\begin{aligned}
h_2(|p_t|) &= \int \frac{q_t^2 dq_t}{4\pi^2} \left\{ \frac{16\pi\beta}{3(Q_1^2 - \mu^2)} [F_2(|p_t|, |q_t|, \mu) - F_2(|p_t|, |q_t|, Q_1)] \tilde{A}(q_t^2) \right. \\
&\quad + 8\pi\kappa F_3(|p_t|, |q_t|) \frac{1}{p_t^2} \tilde{C}(q_t^2) + \frac{16\pi\beta}{3(Q_1^2 - \mu^2)} [F_4(|p_t|, |q_t|, \mu) \\
&\quad \left. - F_4(|p_t|, |q_t|, Q_1)] \frac{1}{p_t^2} \tilde{D}(q_t^2) - 8\pi\kappa F_1(|p_t|, |q_t|) \tilde{C}(p_t^2) \right\}, \tag{47}
\end{aligned}$$

$$\begin{aligned}
h_3(|p_t|) &= \int \frac{q_t^2 dq_t}{4\pi^2} \left\{ 8\pi\kappa F_1(|p_t|, |q_t|) \tilde{A}(q_t^2) + \frac{32\pi\beta W_p}{3(Q_1^2 - \mu^2)} [F_2(|p_t|, |q_t|, \mu) \right. \\
&\quad - F_2(|p_t|, |q_t|, Q_1)] \tilde{A}(q_t^2) - 8\pi\kappa F_5(|p_t|, |q_t|) \frac{1}{p_t^2} \tilde{D}(q_t^2) + \frac{16\pi\beta}{3(Q_1^2 - \mu^2)} \\
&\quad [F_4(|p_t|, |q_t|, \mu) - F_4(|p_t|, |q_t|, Q_1)] \frac{1}{p_t^2} [\tilde{C}(q_t^2) + 2W_p \tilde{D}(q_t^2)] \\
&\quad \left. - 8\pi\kappa F_1(|p_t|, |q_t|) [-\tilde{A}(p_t^2) + p_t^2 \tilde{D}(p_t^2)] \right\}, \tag{48}
\end{aligned}$$

$$\begin{aligned}
h_4(|p_t|) &= \int \frac{q_t^2 dq_t}{4\pi^2} \left\{ \frac{-16\pi\beta}{3(Q_1^2 - \mu^2)} [F_2(|p_t|, |q_t|, \mu) - F_2(|p_t|, |q_t|, Q_1)] \tilde{A}(q_t^2) \right. \\
&\quad + 8\pi\kappa F_3(|p_t|, |q_t|) \frac{1}{p_t^2} \tilde{C}(q_t^2) - \frac{16\pi\beta}{3(Q_1^2 - \mu^2)} [F_4(|p_t|, |q_t|, \mu) \\
&\quad \left. - F_4(|p_t|, |q_t|, Q_1)] \frac{1}{p_t^2} \tilde{D}(q_t^2) - 8\pi\kappa F_1(|p_t|, |q_t|) \tilde{C}(p_t^2) \right\}. \tag{49}
\end{aligned}$$

The B-S scalar functions  $\tilde{A}(p_t^2)$ ,  $\tilde{C}(p_t^2)$  and  $\tilde{D}(p_t^2)$  should be normalized such that they satisfy Eq.(45).

## V. Numerical solutions for the B-S wave function

In this section we solve the three coupled integral equations, Eqs.(37), (38) and (39), numerically. The method is to discretize the integration region into  $n$  pieces (with  $n$  sufficiently large). In this way, the integral equations become matrix equations and the B-S scalar functions  $\tilde{A}(p_t^2)$ ,  $\tilde{C}(p_t^2)$  and  $\tilde{D}(p_t^2)$  become  $n$  dimensional vectors. The matrix equations obtained in this way can be written in the following form,

$$\tilde{A} = Z_1 \tilde{A} + Z_2 \tilde{C} + Z_3 \tilde{D}, \tag{50}$$

$$R_1 \tilde{A} + R_2 \tilde{C} + R_3 \tilde{D} = 0, \tag{51}$$

$$T_1\tilde{A} + T_2\tilde{C} + T_3\tilde{D} = 0, \quad (52)$$

where  $Z_i, R_i, T_i (i = 1, 2, 3)$  are  $n \times n$  matrices and are given by Eqs. (37), (38) and (39).

Substituting Eqs.(51) and (52) into (50) we obtain the eigenvalue equation for  $\tilde{A}$

$$H\tilde{A} = \tilde{A}, \quad (53)$$

where  $H$  is an  $n \times n$  matrix

$$H = Z_1 + Z_2(T_3^{-1}T_2 - R_3^{-1}R_2)^{-1}(R_3^{-1}R_1 - T_3^{-1}T_1) + Z_3(T_2^{-1}T_3 - R_2^{-1}R_3)^{-1}(R_2^{-1}R_1 - T_2^{-1}T_1). \quad (54)$$

The eigenvalue equation (53) is solved by the so-called inverse iteration method[18].

In this way, we first construct the operator

$$K = \frac{1}{H - \lambda}, \quad (55)$$

where  $\lambda$  is some parameter which is chosen to be near to the eigenvalue 1 in Eq.(53).

In order to solve for the eigenvector  $\tilde{A}$ , we start with an arbitrary vector  $Y$  and operate  $K$  on  $Y$  sufficiently many times so that the eigenvector corresponding to the eigenvalue 1 dominates. In this way, the scalar function  $\tilde{A}$  is obtained.

In our model we have several parameters,  $\alpha_s^{(\text{eff})}$ ,  $\kappa$ ,  $Q_1^2$ ,  $m_D$  and  $E_0$ . The parameter  $Q_1^2$  has been described in Section III, with  $Q_1^2 = 3.2\text{GeV}^2$  from the data of the electromagnetic form factor of the proton. It is noted that this value corresponds to the  $(qq')$  axial vector diquark ( $q, q' = u$  or  $d$ ), i.e., for  $\Sigma_Q^{(*)}$ . In the cases of  $\Xi_Q^{(*)}$  or  $\Omega_Q^{(*)}$  this value might be somewhat different because of  $SU(3)$  flavor symmetry breaking. However, we do not have data to extract  $Q_1^2$  for  $\Xi_Q^{(*)}$  and  $\Omega_Q^{(*)}$  at present. In this work, we simply use the same value for  $Q_1^2$  based on the approximate  $SU(3)$  flavor symmetry. On the other hand, the binding energy should satisfy the following relation

$$m_{\omega_Q^{(*)}} = m_Q + m_D + E_0, \quad (56)$$

where we have omitted corrections of  $O(1/m_Q)$ , since we are working in the heavy quark limit. Note that  $m_D + E_0$  is independent of the flavor of the heavy quark, because of the  $SU(2)_f \times SU(2)_s$  symmetry. From the B-S equation solutions in the meson case, it has been found that the values  $m_b = 5.02\text{GeV}$  and  $m_c = 1.58\text{GeV}$  give predictions which are in good agreement with experiments [15]. Hence in the baryon case we expect

$$m_D + E_0 = 0.88\text{GeV}(\text{for } \Sigma_Q^{(*)}), \quad 1.07\text{GeV}(\text{for } \Xi_Q^{(*)}), \quad 1.12\text{GeV}(\text{for } \Omega_Q^{(*)}). \quad (57)$$

The parameter  $m_D$  cannot be determined, although there are suggestions from the analysis of valence structure functions that it should be around  $0.9\text{GeV}$  for non-strange diquarks [19]. Hence we let it vary within some reasonable range. When we solve the eigenvalue equation Eq.(53), the condition that the eigenvalue is 1 provides a relation between  $\alpha_{\text{seff}}$  and  $\kappa$ . As discussed in Ref.[9]  $\kappa$  is related to  $\kappa'$  ( $\kappa'$  is the confinement parameter in the heavy meson case and is about  $0.2\text{GeV}^2$ [14, 15]), where  $\kappa \sim \Lambda_{\text{QCD}}\kappa'$ . Therefore, in our numerical calculations we let  $\kappa$  vary in the region between  $0.02\text{GeV}^3$  and  $0.1\text{GeV}^3$ . The diquark mass,  $m_D$ , is chosen to vary from  $0.9\text{GeV}$  to  $1\text{GeV}$  for  $\Sigma_Q^{(*)}$ , from  $1.1\text{GeV}$  to  $1.2\text{GeV}$  for  $\Xi_Q^{(*)}$ , and from  $1.15\text{GeV}$  to  $1.25\text{GeV}$  for  $\Omega_Q^{(*)}$ . Then we obtain the parameter  $\alpha_s^{(\text{eff})}$  for different values of  $m_D$  and  $\kappa$ . The numerical results are shown in Tables 1,2 and 3 for  $\Sigma_Q^{(*)}$ ,  $\Xi_Q^{(*)}$  and  $\Omega_Q^{(*)}$ , respectively.

With the parameters in Tables 1,2 and 3 we obtain the numerical solution for the B-S scalar function  $\tilde{A}$  as the eigenvector of Eq.(53). Consequently, we get the numerical solutions for  $\tilde{C}$  and  $\tilde{D}$  from Eqs.(51) and (52). These solutions depend on the parameters  $m_D$  and  $\kappa$ . In Figs. 2, 3 and 4 we show the shapes of  $\tilde{A}$ ,  $\tilde{C}$  and  $\tilde{D}$  for  $\Sigma_Q^{(*)}$ ,  $\Xi_Q^{(*)}$  and  $\Omega_Q^{(*)}$  respectively. Figs. 2(a), 3(a) and 4(a) show the dependence on  $\kappa$  for a typical  $m_D$ , while Figs. 2(b), 3(b) and 4(b) show the dependence on  $m_D$  for a typical  $\kappa$ . It can be seen from these figures that for different heavy baryons the shape of the B-S scalar functions are rather similar. This arises from the approximate

Table 1: Values of  $\kappa$  and  $\alpha_s^{(\text{eff})}$  for  $\Sigma_Q^{(*)}$  with three sets of  $m_D$

$m_D(\text{GeV})$	0.90				
$\kappa(\text{GeV}^3)$	0.02	0.04	0.06	0.08	0.10
$\alpha_s^{(\text{eff})}$	0.5190	0.5593	0.5842	0.6061	0.6149
$m_D(\text{GeV})$	0.95				
$\kappa(\text{GeV}^3)$	0.02	0.04	0.06	0.08	0.10
$\alpha_s^{(\text{eff})}$	0.5889	0.6123	0.6285	0.6406	0.6502
$m_D(\text{GeV})$	1.0				
$\kappa(\text{GeV}^3)$	0.02	0.04	0.06	0.08	0.10
$\alpha_s^{(\text{eff})}$	0.6414	0.6560	0.6669	0.6757	0.6828

Table 2: Values of  $\kappa$  and  $\alpha_s^{(\text{eff})}$  for  $\Xi_Q^{(*)}$  with three sets of  $m_D$

$m_D(\text{GeV})$	1.10				
$\kappa(\text{GeV}^3)$	0.02	0.04	0.06	0.08	0.10
$\alpha_s^{(\text{eff})}$	0.5047	0.5402	0.5643	0.5826	0.5974
$m_D(\text{GeV})$	1.15				
$\kappa(\text{GeV}^3)$	0.02	0.04	0.06	0.08	0.10
$\alpha_s^{(\text{eff})}$	0.5785	0.5995	0.6155	0.6283	0.6391
$m_D(\text{GeV})$	1.20				
$\kappa(\text{GeV}^3)$	0.02	0.04	0.06	0.08	0.10
$\alpha_s^{(\text{eff})}$	0.6341	0.6478	0.6588	0.6682	0.6763

Table 3: Values of  $\kappa$  and  $\alpha_s^{(\text{eff})}$  for  $\Omega_Q^{(*)}$  with three sets of  $m_D$

$m_D(\text{GeV})$	1.15				
$\kappa(\text{GeV}^3)$	0.02	0.04	0.06	0.08	0.10
$\alpha_s^{(\text{eff})}$	0.4975	0.5325	0.5565	0.5748	0.5897
$m_D(\text{GeV})$	1.20				
$\kappa(\text{GeV}^3)$	0.02	0.04	0.06	0.08	0.10
$\alpha_s^{(\text{eff})}$	0.5729	0.5935	0.6093	0.6222	0.6331
$m_D(\text{GeV})$	1.25				
$\kappa(\text{GeV}^3)$	0.02	0.04	0.06	0.08	0.10
$\alpha_s^{(\text{eff})}$	0.6296	0.6430	0.6539	0.6633	0.6714

$SU(3)$  flavor symmetry and is to be expected. All the scalar functions decrease to zero when  $|p_t|$  is larger than about 1.5 GeV, because of the confinement interaction. Furthermore, since we are discussing the ground states  $\omega_Q^{(*)}$ , there are no nodes in the functions.

## VI. Application to the nonleptonic decays $\Omega_b \rightarrow \Omega_c^{(*)} P (V)$

In this section we will apply the numerical solutions of the B-S equation to the nonleptonic decays  $\Omega_b \rightarrow \Omega_c^{(*)}$  and a pseudoscalar or vector meson. In fact,  $\Sigma_b^{(*)}$  and  $\Xi_b^{(*)}$  decay strongly and their weak decays are hard to observe. However,  $\Omega_b$  decays only weakly. We will first calculate the Isgur-Wise functions  $\xi(\omega)$  and  $\zeta(\omega)$  for  $\Omega_b^{(*)} \rightarrow \Omega_c^{(*)}$  in Eq.(40) and then apply them to the nonleptonic weak decays of  $\Omega_b$ .

### A. Isgur-Wise functions for $\Omega_b^{(*)} \rightarrow \Omega_c^{(*)}$

The Isgur-Wise functions  $\xi(\omega)$  and  $\zeta(\omega)$  are related to the overlap integrals of the B-S wave functions of the initial ( $\Omega_b$ ) and final ( $\Omega_c^{(*)}$ ) states. The concrete expression for them can be obtained by comparing the structure  $\bar{B}_{m'}^\mu(v')\Gamma B_{m\mu}(v)$  and  $v \cdot \bar{B}_{m'}(v')\Gamma v' \cdot B_m(v)$  on both sides of Eq.(40). Similarly to Eq.(44), we have the following equation after substituting Eq.(7) into Eq.(42) and using Eq.(40)

$$\begin{aligned} \bar{B}_{m'}^\nu(v')\Gamma B_m^\mu(v)(\xi(\omega)g_{\mu\nu} + \zeta(\omega)v_\nu v'_\mu) &= \int \frac{d^4p}{(2\pi)^4} \frac{i}{p_l + E_0 + m_D + i\epsilon} \bar{\chi}_{Pm'}^\mu(p')\Gamma \\ &\int \frac{d^4q}{(2\pi)^4} G_{\mu\nu}(P, p, q)\chi_{Pm}^\nu(p). \end{aligned} \quad (58)$$

Substituting Eq.(17) and Eq.(18) into Eq.(58) and using Eqs.(24), (25) and (26), we find that on the right hand side of Eq.(58) there are the following structures:  $p'_t \cdot \bar{B}_{m'}(v')\Gamma v' \cdot B_m(v)$ ,  $v \cdot \bar{B}_{m'}(v')\Gamma p_t \cdot B_m(v)$ ,  $p'_t \cdot \bar{B}_{m'}(v')\Gamma p_t \cdot B_m(v)$ ,  $p_t \cdot \bar{B}_{m'}(v')\Gamma p_t \cdot B_m(v)$ , and  $p'_t \cdot \bar{B}_{m'}(v')\Gamma p'_t \cdot B_m(v)$ . However, all of them can be expressed in terms of  $\bar{B}_{m'}^\mu(v')\Gamma B_{m\mu}(v)$  and  $v \cdot \bar{B}_{m'}(v')\Gamma v' \cdot B_m(v)$ , after the integration over  $p$ , on the

grounds of Lorentz invariance. Take  $p'_t \cdot \bar{B}_{m'}(v') \Gamma p_t \cdot B_{m\mu}(v)$  as an example. In general, the integral  $\int \frac{d^4 q}{(2\pi)^4} p_t'^\mu p_t^\nu f$ , where  $f$  is some Lorentz scalar function, can be expressed in terms of  $g^{\mu\nu}$ ,  $v^\mu v^\nu$ ,  $v'^\mu v^\nu$ ,  $v'^\mu v'^\nu$  and  $v^\mu v'^\nu$ . However, only the  $g^{\mu\nu}$  and  $v^\mu v'^\nu$  terms contribute when contracted with  $\bar{B}_{m'\mu}(v') \Gamma B_{m\nu}(v)$ , leading to the structures  $\bar{B}_{m'}^\mu(v') \Gamma B_{m\mu}(v)$  and  $v \cdot \bar{B}_{m'}(v') \Gamma v' \cdot B_m(v)$ , respectively. The coefficients of these two terms can be obtained directly. In this way, we have the following replacement rule:

$$\begin{aligned}
p'_t \cdot \bar{B}_{m'}(v') \Gamma v' \cdot B_m(v) &\rightarrow \frac{1}{1-\omega^2} v \cdot p'_t v \cdot \bar{B}_{m'}(v') \Gamma v' \cdot B_m(v), \\
v \cdot \bar{B}_{m'}(v') \Gamma p_t \cdot B_m(v) &\rightarrow \frac{1}{1-\omega^2} v' \cdot p_t v \cdot \bar{B}_{m'}(v') \Gamma v' \cdot B_m(v), \\
p'_t \cdot \bar{B}_{m'}(v') \Gamma p_t \cdot B_m(v) &\rightarrow \left[ \frac{1}{2} p_t \cdot p'_t - \frac{\omega}{2(\omega^2-1)} v \cdot p'_t v' \cdot p_t \right] \bar{B}_{m'}^\mu(v') \Gamma B_{m\mu}(v) \\
&\quad + \left[ -\frac{\omega}{2(\omega^2-1)} p_t \cdot p'_t + \frac{\omega^2+2}{2(\omega^2-1)^2} v \cdot p'_t v' \cdot p_t \right] v \cdot \bar{B}_{m'}(v') \Gamma v' \cdot B_m(v), \\
p_t \cdot \bar{B}_{m'}(v') \Gamma p_t \cdot B_m(v) &\rightarrow \left[ -\frac{1}{2} p_t^2 + \frac{1}{2(\omega^2-1)} (v' \cdot p_t)^2 \right] \bar{B}_{m'}^\mu(v') \Gamma B_{m\mu}(v) \\
&\quad + \left[ \frac{\omega}{2(\omega^2-1)} p_t^2 - \frac{3\omega}{2(\omega^2-1)^2} (v' \cdot p_t)^2 \right] v \cdot \bar{B}_{m'}(v') \Gamma v' \cdot B_m(v), \\
p'_t \cdot \bar{B}_{m'}(v') \Gamma p'_t \cdot B_m(v) &\rightarrow \left[ -\frac{1}{2} p_t'^2 + \frac{1}{2(\omega^2-1)} (v \cdot p'_t)^2 \right] \bar{B}_{m'}^\mu(v') \Gamma B_{m\mu}(v) \\
&\quad + \left[ \frac{\omega}{2(\omega^2-1)} p_t'^2 - \frac{3\omega}{2(\omega^2-1)^2} (v \cdot p'_t)^2 \right] v \cdot \bar{B}_{m'}(v') \Gamma v' \cdot B_m(v). \quad (59)
\end{aligned}$$

Since in the weak transition the diquark acts as a spectator its momentum in the initial and final baryons should be the same,  $p_2 = p'_2$ . Then we can show that

$$p' = p + m_D(v' - v), \quad (60)$$

where we have omitted the  $O(1/m_Q)$  corrections. From Eq. (60) we have the following relations straightforwardly

$$\begin{aligned}
p'_l &= p_l \omega - p_t \sqrt{\omega^2 - 1} \cos \theta, \\
p_t'^2 &= p_t^2 + p_t^2 (\omega^2 - 1) \cos^2 \theta + p_l^2 (\omega^2 - 1) - 2 p_l p_t \omega \sqrt{\omega^2 - 1} \cos \theta,
\end{aligned}$$

$$\begin{aligned}
v' \cdot p_t &= -p_t \sqrt{\omega^2 - 1} \cos \theta, \\
v \cdot p'_t &= (1 - \omega^2) p_l + \omega p_t \sqrt{\omega^2 - 1} \cos \theta, \\
p_t \cdot p'_t &= -p_t^2 - p_t^2 (\omega^2 - 1) \cos^2 \theta + \omega \sqrt{\omega^2 - 1} p_l p_t \cos \theta,
\end{aligned} \tag{61}$$

where  $\theta$  is the angle between  $p_t$  and  $v'_t$ .

With the aid of the relations between  $A(p)$ ,  $C(p)$ ,  $D(p)$  and  $\tilde{A}(p_t^2)$ ,  $\tilde{C}(p_t^2)$ ,  $\tilde{D}(p_t^2)$  [Eqs.(32)-(34)] and using Eqs.(59), (61) and the integration formulae in Appendix A we have the explicit expressions for  $\xi(\omega)$  and  $\zeta(\omega)$  after integrating the  $p_l$  component by selecting the proper contour,

$$\begin{aligned}
\xi(\omega) &= \int \frac{p_t^2 dp_t}{4\pi^2} \int_0^\pi \sin \theta d\theta \frac{-1}{2W_p(E_0 + m_D - W_p)(E_0 + m_D - \omega W_p - p_t \sqrt{\omega^2 - 1} \cos \theta)} \\
&\quad \left\{ -2W_p(E_0 + m_D - W_p)F_A(p_t^2, \cos \theta)\tilde{A}(p_t^2) - \frac{3}{4}(1 - \cos^2 \theta)[h_1(|p_t|) - h_3(|p_t|)] \right. \\
&\quad F_A(p_t^2, \cos \theta) - \frac{1}{2}\omega p_t^2(1 - \cos^2 \theta)F_C(p_t^2, \cos \theta)h_2(|p_t|) + \frac{3}{4}p_t \sqrt{\omega^2 - 1}(1 - \cos^2 \theta) \\
&\quad \cos \theta[h_1(|p_t|) - h_3(|p_t|)]F_C(p_t^2, \cos \theta) + W_p(1 - \cos^2 \theta)(E_0 + m_D - W_p)p_t^2 \tilde{A}(p_t^2) \\
&\quad F_D(p_t^2, \cos \theta) - \frac{1}{2}p_t^2(1 - \cos^2 \theta)[(\omega^2 - 1)W_p + \omega p_t \sqrt{\omega^2 - 1} \cos \theta]h_2(|p_t|) \\
&\quad F_D(p_t^2, \cos \theta) + \frac{3}{4}(1 - \cos^2 \theta)[p_t^2 + p_t^2(\omega^2 - 1)\cos^2 \theta + \omega \sqrt{\omega^2 - 1}W_p p_t] \\
&\quad \left. F_D(p_t^2, \cos \theta)[h_1(|p_t|) - h_3(|p_t|)] \right\},
\end{aligned} \tag{62}$$

and

$$\begin{aligned}
\zeta(\omega) &= \int \frac{p_t^2 dp_t}{4\pi^2} \int_0^\pi \sin \theta d\theta \frac{-1}{2W_p(E_0 + m_D - W_p)(E_0 + m_D - \omega W_p - p_t \sqrt{\omega^2 - 1} \cos \theta)} \\
&\quad \left\{ \frac{1}{\sqrt{\omega^2 - 1}} p_t \cos \theta F_A(p_t^2, \cos \theta)h_2(|p_t|) + \frac{3\omega}{4(\omega^2 - 1)}(1 - 3\cos^2 \theta) \right. \\
&\quad [h_1(|p_t|) - h_3(|p_t|)]F_A(p_t^2, \cos \theta) + \left[ W_p + \frac{\omega}{\sqrt{\omega^2 - 1}} p_t \cos \theta \right] F_C(p_t^2, \cos \theta) \\
&\quad 2W_p(E_0 + m_D - W_p)\tilde{A}(p_t^2) + \frac{\omega}{2(\omega^2 - 1)}[\omega p_t^2 - 3\omega \cos^2 \theta p_t^2 \\
&\quad - 2W_p p_t \sqrt{\omega^2 - 1} \cos \theta]F_C(p_t^2, \cos \theta)h_2(|p_t|) - \frac{3}{4\sqrt{\omega^2 - 1}}[\omega p_t - 3\omega \cos^2 \theta p_t \\
&\quad - 2W_p \sqrt{\omega^2 - 1} \cos \theta] \cos \theta[h_1(|p_t|) - h_3(|p_t|)]F_C(p_t^2, \cos \theta) + [-\omega W_p^2 \\
&\quad \left. - \frac{2\omega^2}{\sqrt{\omega^2 - 1}} W_p p_t \cos \theta - \frac{\omega(2\omega^2 + 1)}{2(\omega^2 - 1)} p_t^2 \cos^2 \theta + \frac{\omega}{2(\omega^2 - 1)} p_t^2 \right]
\end{aligned}$$

$$\begin{aligned}
& [-2W_p(E_0 + m_D - W_p)]F_D(p_t^2, \cos\theta)\tilde{A}(p_t^2) + \frac{1}{2\sqrt{\omega^2 - 1}}[\omega p_t^2 - 3\omega\cos^2\theta p_t^2 \\
& - 2W_p p_t \sqrt{\omega^2 - 1}\cos\theta](\sqrt{\omega^2 - 1}W_p + \omega p_t \cos\theta)F_D(p_t^2, \cos\theta)h_2(|p_t|) \\
& - \frac{3}{4(\omega^2 - 1)}[\omega p_t - 3\omega\cos^2\theta p_t - 2W_p \sqrt{\omega^2 - 1}\cos\theta][p_t + p_t(\omega^2 - 1)\cos^2\theta \\
& + \omega\sqrt{\omega^2 - 1}W_p \cos\theta]F_D(p_t^2, \cos\theta)[h_1(|p_t|) - h_3(|p_t|)]\Big\}, \tag{63}
\end{aligned}$$

where  $h_i(|p_t|)$  ( $i = 1, 2, 3, 4$ ) are given in Eqs.(46)-(49) and  $F_A(p_t^2, \cos\theta)$ ,  $F_C(p_t^2, \cos\theta)$  and  $F_D(p_t^2, \cos\theta)$  have the following expressions

$$\begin{aligned}
F_A(p_t^2, \cos\theta) = & \int \frac{q_t^2 dq_t}{4\pi^2} \left\{ 8\pi\kappa F_1(|p'_t|, |q_t|)[\tilde{A}(q_t^2) - \frac{1}{2}q_t^2 \tilde{D}(q_t^2) - \tilde{A}(p_t'^2)] + \frac{16\pi\beta}{3(Q_1^2 - \mu^2)} \right. \\
& [F_2(|p'_t|, |q_t|, \mu) - F_2(|p'_t|, |q_t|, Q_1)][2(\omega W_p + p_t \sqrt{\omega^2 - 1}\cos\theta) \\
& (\tilde{A}(q_t^2) - \frac{1}{2}q_t^2 \tilde{D}(q_t^2)) - \frac{1}{2}q_t^2 \tilde{C}(q_t^2)] + \frac{1}{2p_t'^2} \frac{16\pi\beta}{3(Q_1^2 - \mu^2)} [-F_4(|p'_t|, |q_t|, \mu) \\
& + F_4(|p'_t|, |q_t|, Q_1)][\tilde{C}(q_t^2) + 2(\omega W_p + p_t \sqrt{\omega^2 - 1}\cos\theta)\tilde{D}(q_t^2)] \\
& \left. + \frac{1}{2p_t'^2} 8\pi\kappa F_5(|p'_t|, |q_t|)\tilde{D}(q_t^2) \right\}, \tag{64}
\end{aligned}$$

$$\begin{aligned}
F_C(p_t^2, \cos\theta) = & \frac{1}{m_D^2} \int \frac{q_t^2 dq_t}{4\pi^2} \left\{ 8\pi\kappa F_1(|p'_t|, |q_t|)[(\omega W_p + p_t \sqrt{\omega^2 - 1}\cos\theta)(\tilde{A}(q_t^2) - \tilde{A}(p_t'^2) \right. \\
& + p_t'^2 \tilde{D}(p_t'^2)) + ((\omega W_p + p_t \sqrt{\omega^2 - 1}\cos\theta)^2 - m_D^2)\tilde{C}(p_t'^2)] + \frac{16\pi\beta}{3(Q_1^2 - \mu^2)} \\
& [F_2(|p'_t|, |q_t|, \mu) - F_2(|p'_t|, |q_t|, Q_1)][(\omega W_p + p_t \sqrt{\omega^2 - 1}\cos\theta)^2 + m_D^2] \\
& \tilde{A}(q_t^2) - \frac{1}{p_t'^2} 8\pi\kappa F_3(|p'_t|, |q_t|)[(\omega W_p + p_t \sqrt{\omega^2 - 1}\cos\theta)^2 - m_D^2]\tilde{C}(q_t^2) \\
& - \frac{1}{p_t'^2} \frac{16\pi\beta}{3(Q_1^2 - \mu^2)} [-F_4(|p'_t|, |q_t|, \mu) + F_4(|p'_t|, |q_t|, Q_1)][(\omega W_p \\
& + p_t \sqrt{\omega^2 - 1}\cos\theta)\tilde{C}(q_t^2) + ((\omega W_p + p_t \sqrt{\omega^2 - 1}\cos\theta)^2 + m_D^2)\tilde{D}(q_t^2)] \\
& \left. - \frac{1}{p_t'^2} 8\pi\kappa F_5(|p'_t|, |q_t|)(\omega W_p + p_t \sqrt{\omega^2 - 1}\cos\theta)\tilde{D}(q_t^2) \right\}, \tag{65}
\end{aligned}$$

$$\begin{aligned}
F_D(p_t^2, \cos\theta) = & -\frac{1}{m_D^2} \int \frac{q_t^2 dq_t}{4\pi^2} \left\{ 8\pi\kappa F_1(|p'_t|, |q_t|) \left[ \tilde{A}(q_t^2) + \frac{m_D^2}{2p_t'^2} q_t^2 \tilde{D}(q_t^2) - \tilde{A}(p_t'^2) \right. \right. \\
& + (\omega W_p + p_t \sqrt{\omega^2 - 1}\cos\theta)\tilde{C}(p_t'^2) + (p_t'^2 + m_D^2)\tilde{D}(p_t'^2) \Big] + \frac{16\pi\beta}{3(Q_1^2 - \mu^2)} \\
& [F_2(|p'_t|, |q_t|, \mu) - F_2(|p'_t|, |q_t|, Q_1)] \left[ (\omega W_p + p_t \sqrt{\omega^2 - 1}\cos\theta) (\tilde{A}(q_t^2) \right. \\
& \left. + \frac{m_D^2}{p_t'^2} q_t^2 \tilde{D}(q_t^2)) + \frac{m_D^2}{2p_t'^2} q_t^2 \tilde{C}(q_t^2) \right] - \frac{1}{p_t'^2} 8\pi\kappa F_3(|p'_t|, |q_t|)(\omega W_p \\
& + p_t \sqrt{\omega^2 - 1}\cos\theta)\tilde{D}(q_t^2) \Big\}
\end{aligned}$$



$$\begin{aligned}
& +p_t\sqrt{\omega^2-1}\cos\theta)\tilde{C}(q_t^2) - \frac{1}{p_t'^2} \frac{16\pi\beta}{3(Q_1^2-\mu^2)} [-F_4(|p_t'|, |q_t|, \mu) \\
& + F_4(|p_t'|, |q_t|, Q_1)] \left[ \frac{3m_D^2 + 2p_t'^2}{2p_t'^2} (\tilde{C}(q_t^2) + 2(\omega W_p + p_t\sqrt{\omega^2-1}\cos\theta) \right. \\
& \left. \tilde{D}(q_t^2)) - (\omega W_p + p_t\sqrt{\omega^2-1}\cos\theta)\tilde{D}(q_t^2) \right] - \frac{3m_D^2 + 2p_t'^2}{2p_t'^2} \\
& 8\pi\kappa F_5(|p_t'|, |q_t|)[\tilde{D}(q_t^2)] \}. \tag{66}
\end{aligned}$$

In Section V we obtained the numerical results for  $\tilde{A}(p_t^2)$ ,  $\tilde{C}(p_t^2)$ , and  $\tilde{D}(p_t^2)$ . Substituting these results into Eqs.(62) and (63) we have the numerical solutions for  $\xi(\omega)$  and  $\zeta(\omega)$  depending on the parameters in our model. For  $\Omega_b^{(*)} \rightarrow \Omega_c^{(*)}$ , we show the Isgur-Wise functions with typical value  $m_D = 1.20\text{GeV}$  in Fig.5(a) ( $\kappa = 0.02\text{GeV}^3$ ) and Fig.5(b) ( $\kappa = 0.10\text{GeV}^3$ ) respectively. The dependence of the Isgur-Wise functions on  $m_D$  are shown in Fig.5(c) ( $m_D = 1.15\text{GeV}$ ) and Fig.5(d) ( $m_D = 1.25\text{GeV}$ ) for  $\kappa = 0.06\text{GeV}^3$ . It can be seen from these plots that  $\xi(\omega)$  and  $\zeta(\omega)$  have opposite signs and  $\xi(\omega)$  changes more rapidly than  $\zeta(\omega)$  as  $\omega$  increases.

It is interesting to study the relation between  $\xi(\omega)$  and  $\zeta(\omega)$ . Based on the picture that in the large  $N_c$  limit heavy baryons are viewed as the bound states of chiral solitons and heavy mesons[20], Chow has shown that  $\xi(\omega)$  and  $\zeta(\omega)$  obey the following relation[21]

$$\xi(\omega) = -(1 + \omega)\zeta(\omega). \tag{67}$$

The deviation from this relation is caused by  $1/N_c$  corrections. From Figs.5(a)-(d) we can see that, in the range of the parameters in our model, Eq.(67) is generally satisfied. For some sets of parameters this relation holds well.

## B. Nonleptonic decays $\Omega_b \rightarrow \Omega_c^{(*)} P (V)$

In this section we will discuss the Cabbibo-allowed two body nonleptonic decays of  $\Omega_b \rightarrow \Omega_c^{(*)} P (V)$  ( $P$  and  $V$  stand for pseudoscalar and vector mesons respec-

tively). The Hamiltonian describing such decays reads

$$H_{\text{eff}} = \frac{G_F}{\sqrt{2}} V_{cb} V_{UD}^* (a_1 O_1 + a_2 O_2), \quad (68)$$

with  $O_1 = (\bar{D}U)(\bar{c}b)$  and  $O_2 = (\bar{c}U)(\bar{D}b)$ , where  $U$  and  $D$  are the fields for light quarks involved in the decay, and  $(\bar{q}_1 q_2) = \bar{q}_1 \gamma_\mu (1 - \gamma_5) q_2$  is understood. The parameters  $a_1$  and  $a_2$  are treated as free parameters since they involve hadronization effects. Since  $\Omega_b$  decays are energetic, the factorization assumption is applied so that one of the currents in the Hamiltonian (68) is factorized out and generates a meson[22, 23]. Thus the decay amplitude of the two body nonleptonic decay becomes the product of two matrix elements, one is related to the decay constant of the factorized meson ( $P$  or  $V$ ) and the other is the weak transition matrix element between  $\Omega_b$  and  $\Omega_c^{(*)}$ ,

$$M^{fac}(\Omega_b \rightarrow \Omega_c^{(*)} P(V)) = \frac{G_F}{\sqrt{2}} V_{cb} V_{UD}^* a_1 \langle P(V) | A_\mu(V_\mu) | 0 \rangle \langle \Omega_c^{(*)}(v') | J^\mu | \Omega_b(v) \rangle. \quad (69)$$

Here  $J_\mu$  is the weak current  $(\bar{c}b)$  and  $\langle 0 | A_\mu(V_\mu) | P(V) \rangle$  are related to the decay constants of the pseudoscalar or vector mesons by

$$\begin{aligned} \langle 0 | A_\mu | P \rangle &= i f_P q_\mu, \\ \langle 0 | V_\mu | V \rangle &= f_V m_V \epsilon_\mu, \end{aligned} \quad (70)$$

where  $q_\mu$  is the momentum of the emitted meson (from the W-boson),  $\epsilon_\mu$  is the polarization vector of the vector meson, and the normalization for the decay constants is chosen so that  $f_\pi = 132 \text{ MeV}$ . It is noted that in the two body nonleptonic weak decays  $\Omega_b \rightarrow \Omega_c^{(*)} P(V)$  there is no contribution from the  $a_2$  term, since such a term corresponds to the transition of  $\Omega_b$  to a light baryon instead of  $\Omega_c^{(*)}$ . On the other hand, the general form for the amplitudes of  $\Omega_b \rightarrow \Omega_c^{(*)} P(V)$  are

$$\begin{aligned} M(\Omega_b \rightarrow \Omega_c P) &= i \bar{u}_f(v') (A + B \gamma_5) u_i(v), \\ M(\Omega_b \rightarrow \Omega_c V) &= \bar{u}_f(v') \epsilon^{*\mu} [A_1 \gamma_\mu \gamma_5 + A_2 p_{f\mu} \gamma_5 + B_1 \gamma_\mu + B_2 p_{f\mu}] u_i(v), \end{aligned}$$

$$\begin{aligned}
M(\Omega_b \rightarrow \Omega_c^* P) &= i q_\mu \bar{u}_f^\mu(v')(C + D\gamma_5)u_i(v), \\
M(\Omega_b \rightarrow \Omega_c^* V) &= \bar{u}_f^\nu(v')\epsilon^{*\mu}[g_{\nu\mu}(C_1 + D_1\gamma_5) + p_{i\nu}\gamma_\mu(C_2 + D_2\gamma_5) \\
&\quad + p_{i\nu}p_{f\mu}(C_3 + D_3\gamma_5)]u_i(v),
\end{aligned} \tag{71}$$

where  $u_i$  is the dirac spinor of  $\Omega_b$ ,  $u_f^{(\mu)}$  is the dirac (Rarita-Schwinger) spinor of  $\Omega_c^{(*)}$ , and  $p_{i(f)}$  is the momentum of  $\Omega_b$  ( $\Omega_c^{(*)}$ ).

From Eqs.(69)-(71) and using Eq.(40) we find

$$\begin{aligned}
A &= \frac{G_F}{\sqrt{2}} V_{cb} V_{UD}^* a_1 f_P \frac{1}{3} (m_i - m_f) [(\omega + 2)\xi(\omega) + (\omega^2 - 1)\zeta(\omega)], \\
B &= \frac{G_F}{\sqrt{2}} V_{cb} V_{UD}^* a_1 f_P \frac{1}{3} (m_i + m_f) [(3\omega - 2)\xi(\omega) + 3(\omega^2 - 1)\zeta(\omega)], \\
A_1 &= B_1 = \frac{G_F}{\sqrt{2}} V_{cb} V_{UD}^* a_1 f_V m_V \frac{1}{3} [\omega\xi(\omega) + (\omega^2 - 1)\zeta(\omega)], \\
A_2 &= \frac{G_F}{\sqrt{2}} V_{cb} V_{UD}^* a_1 f_V m_V \frac{2}{3} \left( \frac{1}{m_i} - \frac{1}{m_f} \right) [\xi(\omega) + (\omega + 1)\zeta(\omega)], \\
B_2 &= -\frac{G_F}{\sqrt{2}} V_{cb} V_{UD}^* a_1 f_V m_V \frac{2}{3} \left( \frac{1}{m_i} + \frac{1}{m_f} \right) [\xi(\omega) + (\omega - 1)\zeta(\omega)], \\
C &= -\frac{G_F}{\sqrt{2}} V_{cb} V_{UD}^* a_1 f_P \frac{1}{\sqrt{3}} \left( 1 + \frac{m_f}{m_i} \right) [\xi(\omega) + (\omega - 1)\zeta(\omega)], \\
D &= -\frac{G_F}{\sqrt{2}} V_{cb} V_{UD}^* a_1 f_P \frac{1}{\sqrt{3}} \left[ \left( 1 - \frac{m_f}{m_i} \right) \xi(\omega) + \left( \omega - 1 - (\omega + 3) \frac{m_f}{m_i} \right) \zeta(\omega) \right], \\
C_1 &= D_1 = \frac{G_F}{\sqrt{2}} V_{cb} V_{UD}^* a_1 f_V m_V \frac{2}{\sqrt{3}} \xi(\omega), \\
C_2 &= -\frac{G_F}{\sqrt{2}} V_{cb} V_{UD}^* a_1 f_V m_V \frac{1}{\sqrt{3}} \frac{1}{m_i} [\xi(\omega) + (\omega + 1)\zeta(\omega)], \\
D_2 &= \frac{G_F}{\sqrt{2}} V_{cb} V_{UD}^* a_1 f_V m_V \frac{1}{\sqrt{3}} \frac{1}{m_i} [\xi(\omega) + (\omega - 1)\zeta(\omega)], \\
C_3 &= D_3 = \frac{G_F}{\sqrt{2}} V_{cb} V_{UD}^* a_1 f_V m_V \frac{2}{\sqrt{3}} \frac{1}{m_i m_f} \zeta(\omega),
\end{aligned} \tag{72}$$

where  $m_i$  ( $m_f$ ) is the mass of  $\Omega_b$  ( $\Omega_c^{(*)}$ ).

With Eqs.(71) and (72) we can calculate the decay widths and polarization parameters for  $\Omega_b \rightarrow \Omega_c^{(*)} P$  ( $V$ ). The kinematic formulae which have been derived using both partial wave and helicity methods can be found in references[24, 25]. These two methods are equivalent. For instance, in the helicity method[25], the

decay width is expressed in terms of the helicity amplitudes,

$$\Gamma = \frac{p_c}{16\pi m_i^2} \sum_{\lambda_i, \lambda_f} |h_{\lambda_f, \lambda_{P(V)}; \lambda_i}|^2, \quad (73)$$

where  $p_c$  is the c.m. momentum of the decay products and the helicity amplitudes are defined as

$$h_{\lambda_f, \lambda_{P(V)}; \lambda_i} = \langle \Omega_c^{(*)}(\lambda_f), P(V)(\lambda_{P(V)}) | H_{\text{eff}} | \Omega_b(\lambda_i) \rangle \quad (\lambda_f - \lambda_{P(V)} = \lambda_i). \quad (74)$$

The “up-down” asymmetry is given by

$$\alpha = \frac{\sum_{\lambda_f} (|h_{\lambda_f, \lambda_{P(V)}; 1/2}|^2 - |h_{\lambda_f, \lambda_{P(V)}; -1/2}|^2)}{\sum_{\lambda_i, \lambda_f} |h_{\lambda_f, \lambda_{P(V)}; \lambda_i}|^2}. \quad (75)$$

The relations between the helicity amplitudes and the amplitudes given in Eq.(71), which we will not list here, can be found in [25, 26]. Then from Eqs.(72)-(75), we obtain the numerical results for the decay widths and asymmetry parameters. In Table 4 we list the results for  $m_D = 1.20\text{GeV}$ . The numbers without (with) brackets correspond to  $\kappa = 0.02\text{GeV}^3$  ( $\kappa = 0.10\text{GeV}^3$ ). The results for  $\kappa = 0.06\text{GeV}^3$  in the range  $m_D = 1.15\text{GeV}$  (without brackets) and  $m_D = 1.25\text{GeV}$  (with brackets) are shown in Table 5. In the calculations we have taken  $m_{\Omega_b} = 6.14\text{GeV}$  and the following decay constants

$$f_\pi = 132\text{MeV}, \quad f_{D_s} = 241\text{MeV}[27], \quad f_\rho = 216\text{MeV}, \quad f_{D_s^*} = f_{D_s^*}.$$

It can be seen from Tables 4 and 5 that the predictions for the decay widths show a strong dependence on the parameters  $\kappa$  and  $m_D$  in our model. The experimental data in the future will be used to fix these parameters and test our model. However, the dependence of the up-down asymmetries on these parameters is slight.

The decay widths and asymmetry parameters have also been calculated in the nonrelativistic quark model approach[26], where the form factors are calculated at the zero-recoil point and then extrapolated to other  $\omega$  values under the assumption

Table 4: Predictions for decay widths and asymmetry parameters for  $\Omega_b^- \rightarrow \Omega_c^{(*)} P (V)$  for  $m_D = 1.20\text{GeV}$ .

Process	$\Gamma(10^{10}s^{-1})$	$\alpha$
$\Omega_b^- \rightarrow \Omega_c^0 \pi^-$	$0.052a_1^2 (0.154a_1^2)$	$-0.67 (-0.70)$
$\Omega_b^- \rightarrow \Omega_c^0 D_s^-$	$0.261a_1^2 (0.592a_1^2)$	$-0.56 (-0.58)$
$\Omega_b^- \rightarrow \Omega_c^0 \rho^-$	$0.073a_1^2 (0.207a_1^2)$	$-0.68 (-0.71)$
$\Omega_b^- \rightarrow \Omega_c^0 D_s^{*-}$	$0.115a_1^2 (0.245a_1^2)$	$-0.73 (-0.74)$
$\Omega_b^- \rightarrow \Omega_c^{*0} \pi^-$	$0.046a_1^2 (0.133a_1^2)$	$-0.61 (-0.58)$
$\Omega_b^- \rightarrow \Omega_c^{*0} D_s^-$	$0.165a_1^2 (0.370a_1^2)$	$-0.54 (-0.52)$
$\Omega_b^- \rightarrow \Omega_c^{*0} \rho^-$	$0.134a_1^2 (0.354a_1^2)$	$0.59 (0.59)$
$\Omega_b^- \rightarrow \Omega_c^{*0} D_s^{*-}$	$0.462a_1^2 (0.960a_1^2)$	$0.31 (0.31)$

Table 5: Predictions for decay widths and asymmetry parameters for  $\Omega_b^- \rightarrow \Omega_c^{(*)} P (V)$  for  $\kappa = 0.06\text{GeV}^3$ .

Process	$\Gamma(10^{10}s^{-1})$	$\alpha$
$\Omega_b^- \rightarrow \Omega_c^0 \pi^-$	$0.075a_1^2 (0.145a_1^2)$	$-0.64 (-0.72)$
$\Omega_b^- \rightarrow \Omega_c^0 D_s^-$	$0.358a_1^2 (0.562a_1^2)$	$-0.54 (-0.59)$
$\Omega_b^- \rightarrow \Omega_c^0 \rho^-$	$0.102a_1^2 (0.150a_1^2)$	$-0.65 (-0.70)$
$\Omega_b^- \rightarrow \Omega_c^0 D_s^{*-}$	$0.149a_1^2 (0.232a_1^2)$	$-0.71 (-0.75)$
$\Omega_b^- \rightarrow \Omega_c^{*0} \pi^-$	$0.067a_1^2 (0.123a_1^2)$	$-0.64 (-0.56)$
$\Omega_b^- \rightarrow \Omega_c^{*0} D_s^-$	$0.227a_1^2 (0.345a_1^2)$	$-0.56 (-0.50)$
$\Omega_b^- \rightarrow \Omega_c^{*0} \rho^-$	$0.200a_1^2 (0.314a_1^2)$	$0.59 (0.59)$
$\Omega_b^- \rightarrow \Omega_c^{*0} D_s^{*-}$	$0.616a_1^2 (0.888a_1^2)$	$0.31 (0.31)$

of a dipole behaviour. By comparing the predictions in the B-S and quark models we find that the decay widths in our model are smaller than those in the quark model. For the asymmetry parameters, the difference is even larger. Except for the processes  $\Omega_b^- \rightarrow \Omega_c^{0*} \pi^-$  and  $\Omega_b^- \rightarrow \Omega_c^{0*} D_s^-$  in Tables 4 and 5, even the signs of  $\alpha$  in these two models are opposite.

## VII. Summary and discussion

Since in the heavy quark limit the light degrees of freedom in a heavy baryon

have good spin and isospin quantum numbers and since the internal structure is blind to the flavor and spin direction of the heavy quark, we assume that a heavy baryon,  $\omega_Q^{(*)}$ , is composed of a heavy quark and a light axial vector diquark. Based on this picture, we establish the B-S equation for the heavy baryon  $\omega_Q^{(*)}$ . We discuss the form of the B-S wave function and find that in the heavy quark limit there are three B-S scalar functions to describe the dynamics inside a heavy baryon  $\omega_Q^{(*)}$ . This is consistent with our physical picture. In order to solve the B-S equation, we assume a kernel containing a scalar confinement term and a one-gluon-exchange term, as in the  $\Lambda_Q$  case. In the heavy quark limit, the heavy quark is almost on mass-shell inside a heavy baryon and it is appropriate to apply the covariant instantaneous approximation in the kernel. Then we derive explicitly three coupled integral equations for the three B-S scalar functions  $\tilde{A}$ ,  $\tilde{C}$  and  $\tilde{D}$ . These equations are solved numerically and we give the model predictions for these functions. The results appear reasonable. It is shown that the shapes of these functions are similar for  $\Sigma_Q^{(*)}$ ,  $\Xi_Q^{(*)}$  and  $\Omega_Q^{(*)}$ , with differences arising from  $SU(3)$  flavor symmetry breaking effects.

Although the B-S equation is formally the exact equation to describe the bound state, there is much difficulty in applying it to the real physical state. The most difficult point is that we must take a phenomenologically inspired form for the kernel. Furthermore, we have used the quark and diquark propagators with their free form, which leads to some uncertainties. In our approach, there are several parameters such as  $\kappa$ ,  $m_D$  and  $\alpha_s^{(\text{eff})}$ , subject to the condition that the observed masses of  $\omega_Q^{(*)}$  be reproduced. In our numerical solutions we let these parameters vary in some reasonable range. Another parameter is  $Q_1^2$ , which arises from the internal structure of diquark. Its value for the  $(qq')$  diquark ( $q, q' = u$  or  $d$ ) is extracted from the data of the electromagnetic form factor of the proton. When there is a strange quark in the diquark, we do not have a means to determine its exact value at present. In

the future, the experimental data for  $\omega_Q^{(*)}$  should help to fix the parameters in our model.

As phenomenological applications, this model has been used to calculate the the Isgur-Wise functions  $\xi(\omega)$  and  $\zeta(\omega)$  for  $\Omega_b^{(*)} \rightarrow \Omega_c^{(*)}$ , and consequently, has provided theoretical predictions for the Cabbibo-allowed two body nonleptonic decay rates and up-down asymmetries for the physical processes  $\Omega_b \rightarrow \Omega_c^{(*)} P (V)$ . It has been shown that the relation between  $\xi(\omega)$  and  $\zeta(\omega)$  in our model is generally consistent with that in the soliton model in the large  $N_c$  limit. We have also compared our model predictions with those in the nonrelativistic quark model. Our model yields decay widths which are much smaller and for the asymmetry parameters the difference is even bigger. All these predictions will be tested in future experiments.

### Acknowledgment:

This work was supported in part by the Australian Research Council and the National Science Foundation of China.

## Appendix A. Integration formulae

In this appendix we give the formulae which are used to reduce the three dimensional integration to the one dimensional integration. In the following formulae  $\phi(q_t^2)$  is some arbitrary function of  $q_t^2$ . The relevant results needed are:

$$I_1 = \int \frac{d^3 q_t}{(2\pi)^3} \frac{\phi(q_t^2)}{[(p_t - q_t)^2 + \mu^2]^2} = \int \frac{q_t^2 dq_t}{4\pi^2} \phi(q_t^2) F_1(|p_t|, |q_t|), \quad (76)$$

with

$$F_1(|p_t|, |q_t|) = \frac{2}{(p_t^2 + q_t^2 + \mu^2)^2 - 4p_t^2 q_t^2}. \quad (77)$$

$$I_2 = \int \frac{d^3 q_t}{(2\pi)^3} \frac{\phi(q_t^2)}{(p_t - q_t)^2 + \delta^2} = \int \frac{q_t^2 dq_t}{4\pi^2} \phi(q_t^2) F_2(|p_t|, |q_t|, \delta), \quad (78)$$

with

$$F_2(|p_t|, |q_t|, \delta) = \frac{1}{2|p_t||q_t|} \ln \frac{(|p_t| + |q_t|)^2 + \delta^2}{(|p_t| - |q_t|)^2 + \delta^2}. \quad (79)$$

$$I_3 = \int \frac{d^3 q_t}{(2\pi)^3} \frac{p_t \cdot q_t \phi(q_t^2)}{[(p_t - q_t)^2 + \mu^2]^2} = \int \frac{q_t^2 dq_t}{4\pi^2} \phi(q_t^2) F_3(|p_t|, |q_t|), \quad (80)$$

with

$$F_3(|p_t|, |q_t|) = \frac{1}{4|p_t||q_t|} \left[ \ln \frac{(|p_t| - |q_t|)^2 + \mu^2}{(|p_t| + |q_t|)^2 + \mu^2} + \frac{4|p_t||q_t|(p_t^2 + q_t^2 + \mu^2)}{(p_t^2 + q_t^2 + \mu^2)^2 - 4p_t^2 q_t^2} \right]. \quad (81)$$

$$I_4 = \int \frac{d^3 q_t}{(2\pi)^3} \frac{(p_t \cdot q_t)^2 \phi(q_t^2)}{(p_t - q_t)^2 + \delta^2} = - \int \frac{q_t^2 dq_t}{4\pi^2} \phi(q_t^2) F_4(|p_t|, |q_t|, \delta), \quad (82)$$

with

$$F_4(|p_t|, |q_t|, \delta) = \frac{p_t^2 + q_t^2 + \delta^2}{2} \left[ 1 + \frac{p_t^2 + q_t^2 + \delta^2}{4|p_t||q_t|} \ln \frac{(|p_t| - |q_t|)^2 + \delta^2}{(|p_t| + |q_t|)^2 + \delta^2} \right]. \quad (83)$$

$$I_5 = \int \frac{d^3 q_t}{(2\pi)^3} \frac{(p_t \cdot q_t)^2 \phi(q_t^2)}{[(p_t - q_t)^2 + \mu^2]^2} = \int \frac{q_t^2 dq_t}{4\pi^2} \phi(q_t^2) F_5(|p_t|, |q_t|), \quad (84)$$

with

$$F_5(|p_t|, |q_t|) = \frac{1}{2} \left[ 1 + \frac{p_t^2 + q_t^2 + \mu^2}{2|p_t||q_t|} \ln \frac{(|p_t| - |q_t|)^2 + \mu^2}{(|p_t| + |q_t|)^2 + \mu^2} + \frac{(p_t^2 + q_t^2 + \mu^2)^2}{(p_t^2 + q_t^2 + \mu^2)^2 - 4p_t^2 q_t^2} \right]. \quad (85)$$



## References

- [1] N. Isgur and M.B. Wise, Phys. Lett. **B232** (1989) 113, **B237** (1990) 527; H. Georgi, Phys. Lett. **B264** (1991) 447; see also M. Neubert, Phys. Rep. **245** (1994) 259 for the review.
- [2] OPAL collaboration, R. Akers et al., Z. Phys. **C69** (1996) 195; Phys. Lett. **B353** (1995) 402; OPAL collaboration, K. Ackerstaff et al., hep-ex/9802002.
- [3] UA1 Collaboration, C. Albarjar et al., Phys. Lett. **B273** (1991) 540.
- [4] CDF Collaboration, F. Abe et al., Phys.Rev. **D47** (1993) 2639.
- [5] S.E. Tzmaris, invited talk presented in the 27th International Conference on High Energy Physics, Glasgow, July 20-27, 1994; P. Abreu et al., Phys. Lett. **B374** (1996) 351.
- [6] CDF Collaboration, F.Abe et al., Phys. Rev. **D55** (1997) 1142.
- [7] C. Caso et al., The Particle Data Group, The Eur. Phys. J. **C3** (1998) 1.
- [8] T. Mannel, W. Roberts and Z. Ryzak, Nucl. Phys. **B355** (1991) 38.
- [9] X.-H. Guo and T. Muta, Phys. Rev. **D54** (1996) 4629; Mod. Phys. Lett. **A11** (1996) 1523.
- [10] A. Falk, Nucl. Phys. **B378** (1992) 79.
- [11] T. Mannel, W. Roberts and Z. Ryzak, Phys. Lett. **B271** (1991) 421; W. Roberts, Nucl. Phys. **B389** (1993) 549.
- [12] Y.-B. Dai, X.-H. Guo and C.-S. Huang, Nucl. Phys. **B412** (1994) 277.
- [13] D. Lurie, *Particles and Fields* (Interscience Publishers, John Willey & Sons, New York, London, Sydney, 1968); C. Itzykson and J.B. Zuber, *Quantum Field Theory* (McGraw-Hill, New York, 1980).
- [14] E. Eichten, K. Gottfried, T. Kinoshita, K.D. Lane and T.-M. Yan, Phys. Rev. **D17** (1978) 3090.

- [15] H.-Y. Jin, C.-S. Huang and Y.-B. Dai, Z. Phys. **C56** (1992) 707; Y.-B. Dai, C.-S. Huang and H.-Y. Jin, Z. Phys. **C60** (1993) 527.
- [16] M. Anselmino, P. Kroll and B. Pire, Z. Phys. **C36** (1987) 89; P. Kroll, B. Quadder and W. Schweiger, Nucl. Phys. **B316** (1988) 373.
- [17] G.P. Lepage and S.J. Brodsky, Phys. Rev. **D22** (1980) 2157; S.J. Brodsky, G.P. Lepage, T. Huang and P.B. MacKenzie, in *Particles and Fields 2*, edited by A.Z. Capri and A.N. Kamal (Plenum, New York, 1983), p. 83.
- [18] Y. R. Kwon and F. Tabakin, Phys. Rev. **C18** (1978) 932; C. Savkli and F. Tabakin, hep-ph/9702251.
- [19] F. Close and A.W. Thomas, Phys. Lett. **B212** (1988) 227.
- [20] E. Jenkins, A.V. Manohar and M.B. Wise, Nucl. Phys. **B396** (1993) 27; *ibid.* **B396** (1993) 38; Z. Guralnik, M. Luke and A.V. Manohar, Nucl. Phys. **B390** (1993) 474.
- [21] C.-K. Chow, Phys. Rev. **D51** (1995) 1224; *ibid.* **D54** (1996) 873.
- [22] J.D. Bjorken, Nucl. Phys. (Proc. Suppl.) **11** (1989) 325.
- [23] M.J. Dugan and B. Grinstein, Phys. Lett. **B255** (1991) 583.
- [24] S. Pakvasa, S.F. Tuan and S.P. Rosen, Phys. Rev. **D42** (1990) 3746.
- [25] J.G. Körner and M. Krämer, Z. Phys. **C55** (1992) 659.
- [26] H.-Y. Cheng, Phys. Rev. **D56** (1997) 2799.
- [27] C.T. Sachrajda, CERN-TH-96-257, Talk given at Beauty 96, Rome, Italy, 17-21 Jun 1996. Published in Nucl.Instrum.Meth. **A384** (1996) 26.

## Figure Captions

Fig.1 The vertex of two axial vector diquarks and a gluon.

Fig.2 The B-S scalar wave functions for  $\Sigma_Q^{(*)}$ . The units are:  $\text{GeV}^{-2}$  for  $\tilde{A}(p_t^2)$ ,  $\text{GeV}^{-3}$  for  $\tilde{C}(p_t^2)$  and  $\text{GeV}^{-4}$  for  $\tilde{D}(p_t^2)$ . (a) For  $m_D = 0.95\text{GeV}$ , we show the dependence on  $|p_t|$  for two values of  $\kappa$ . In the upper plane, the upper (lower) solid line is for  $\tilde{A}(p_t^2)$  ( $\tilde{C}(p_t^2)$ ) with  $\kappa = 0.02\text{GeV}^3$ , the upper (lower) dotted line is for  $\tilde{A}(p_t^2)$  ( $\tilde{C}(p_t^2)$ ) with  $\kappa = 0.10\text{GeV}^3$ . In the lower plane, the solid line is for  $\tilde{D}(p_t^2)$  with  $\kappa = 0.02\text{GeV}^3$  and the dotted line is for  $\tilde{D}(p_t^2)$  with  $\kappa = 0.10\text{GeV}^3$ . (b) For  $\kappa = 0.06\text{GeV}^3$ , we show the dependence on  $|p_t|$  for two values of  $m_D$ . In the upper plane, the upper (lower) solid line is for  $\tilde{A}(p_t^2)$  ( $\tilde{C}(p_t^2)$ ) with  $m_D = 0.90\text{GeV}$ , the upper (lower) dotted line is for  $\tilde{A}(p_t^2)$  ( $\tilde{C}(p_t^2)$ ) with  $m_D = 1.00\text{GeV}$ . In the lower plane, the solid line is for  $\tilde{D}(p_t^2)$  with  $m_D = 0.90\text{GeV}$  and the dotted line is for  $\tilde{D}(p_t^2)$  with  $m_D = 1.00\text{GeV}$ .

Fig.3 The B-S scalar wave functions for  $\Xi_Q^{(*)}$ . The units are:  $\text{GeV}^{-2}$  for  $\tilde{A}(p_t^2)$ ,  $\text{GeV}^{-3}$  for  $\tilde{C}(p_t^2)$  and  $\text{GeV}^{-4}$  for  $\tilde{D}(p_t^2)$ . (a) For  $m_D = 1.15\text{GeV}$ , we show the dependence on  $|p_t|$  for two values of  $\kappa$ . In the upper plane, the upper (lower) solid line is for  $\tilde{A}(p_t^2)$  ( $\tilde{C}(p_t^2)$ ) with  $\kappa = 0.02\text{GeV}^3$ , the upper (lower) dotted line is for  $\tilde{A}(p_t^2)$  ( $\tilde{C}(p_t^2)$ ) with  $\kappa = 0.10\text{GeV}^3$ . In the lower plane, the solid line is for  $\tilde{D}(p_t^2)$  with  $\kappa = 0.02\text{GeV}^3$  and the dotted line is for  $\tilde{D}(p_t^2)$  with  $\kappa = 0.10\text{GeV}^3$ . (b) For  $\kappa = 0.06\text{GeV}^3$ , we show the dependence on  $|p_t|$  for two values of  $m_D$ . In the upper plane, the upper (lower) solid line is for  $\tilde{A}(p_t^2)$  ( $\tilde{C}(p_t^2)$ ) with  $m_D = 1.10\text{GeV}$ , the upper (lower) dotted line is for  $\tilde{A}(p_t^2)$  ( $\tilde{C}(p_t^2)$ ) with  $m_D = 1.20\text{GeV}$ . In the lower plane, the solid line is for  $\tilde{D}(p_t^2)$  with  $m_D = 1.10\text{GeV}$  and the dotted line is for  $\tilde{D}(p_t^2)$  with  $m_D = 1.20\text{GeV}$ .

Fig.4 The B-S scalar wave functions for  $\Omega_Q^{(*)}$ . The units are:  $\text{GeV}^{-2}$  for  $\tilde{A}(p_t^2)$ ,  $\text{GeV}^{-3}$  for  $\tilde{C}(p_t^2)$  and  $\text{GeV}^{-4}$  for  $\tilde{D}(p_t^2)$ . (a) For  $m_D = 1.20\text{GeV}$ , we show the dependence on  $|p_t|$  for two values of  $\kappa$ . In the upper plane, the upper (lower) solid

line is for  $\tilde{A}(p_t^2)$  ( $\tilde{C}(p_t^2)$ ) with  $\kappa = 0.02\text{GeV}^3$ , the upper (lower) dotted line is for  $\tilde{A}(p_t^2)$  ( $\tilde{C}(p_t^2)$ ) with  $\kappa = 0.10\text{GeV}^3$ . In the lower plane, the solid line is for  $\tilde{D}(p_t^2)$  with  $\kappa = 0.02\text{GeV}^3$  and the dotted line is for  $\tilde{D}(p_t^2)$  with  $\kappa = 0.10\text{GeV}^3$ . (b) For  $\kappa = 0.06\text{GeV}^3$ , we show the dependence on  $|p_t|$  for two values of  $m_D$ . In the upper plane, the upper (lower) solid line is for  $\tilde{A}(p_t^2)$  ( $\tilde{C}(p_t^2)$ ) with  $m_D = 1.15\text{GeV}$ , the upper (lower) dotted line is for  $\tilde{A}(p_t^2)$  ( $\tilde{C}(p_t^2)$ ) with  $m_D = 1.25\text{GeV}$ . In the lower plane, the solid line is for  $\tilde{D}(p_t^2)$  with  $m_D = 1.15\text{GeV}$  and the dotted line is for  $\tilde{D}(p_t^2)$  with  $m_D = 1.25\text{GeV}$ .

Fig.5(a)-(d) Numerical solutions for  $\xi(\omega)$  and  $\zeta(\omega)$  for  $\Omega_b^{(*)} \rightarrow \Omega_c^{(*)}$ . The upper solid line is  $\xi(\omega)$  and the lower solid line is  $\zeta(\omega)$ . The dotted line is  $-\xi(\omega)/(\omega + 1)$ . The parameters are  $m_D = 1.20\text{GeV}$  and  $\kappa = 0.02\text{GeV}^3$  in (a),  $m_D = 1.20\text{GeV}$  and  $\kappa = 0.10\text{GeV}^3$  in (b),  $\kappa = 0.06\text{GeV}^3$  and  $m_D = 1.15\text{GeV}$  in (c),  $\kappa = 0.06\text{GeV}^3$  and  $m_D = 1.25\text{GeV}$  in (d).

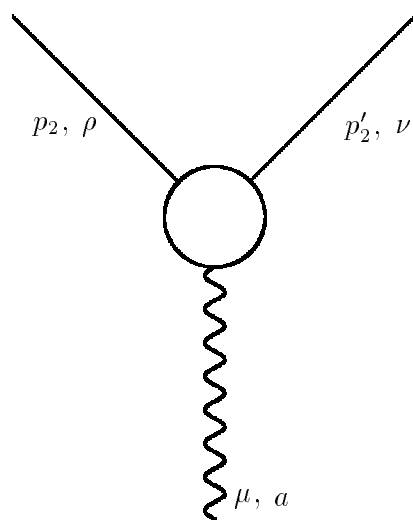


Fig.1

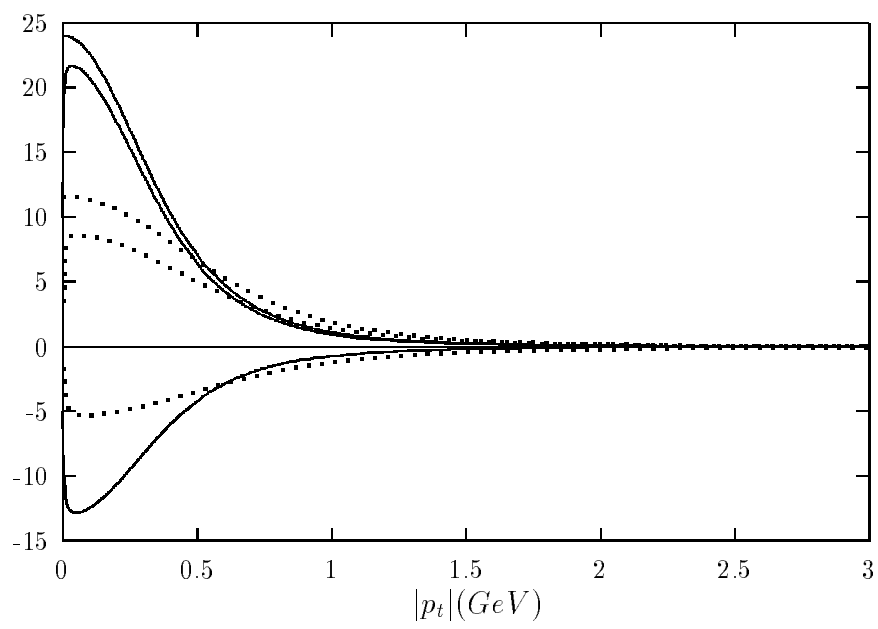


Fig.2(a)

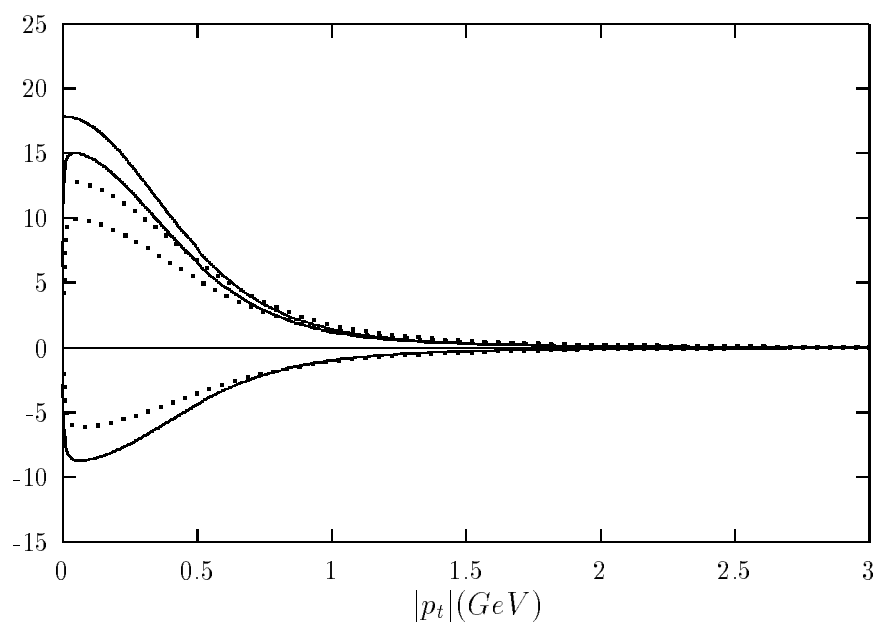


Fig.2(b)

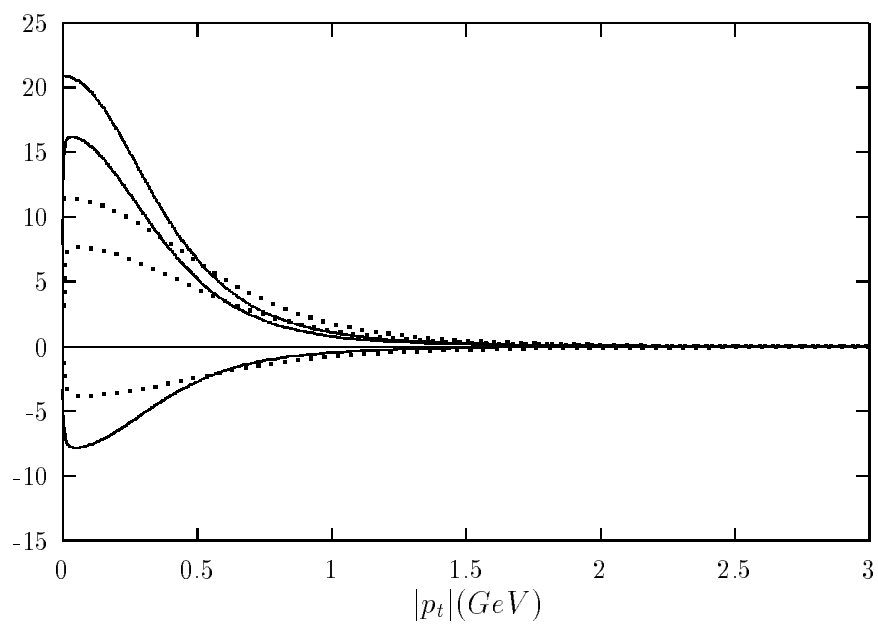


Fig.3(a)

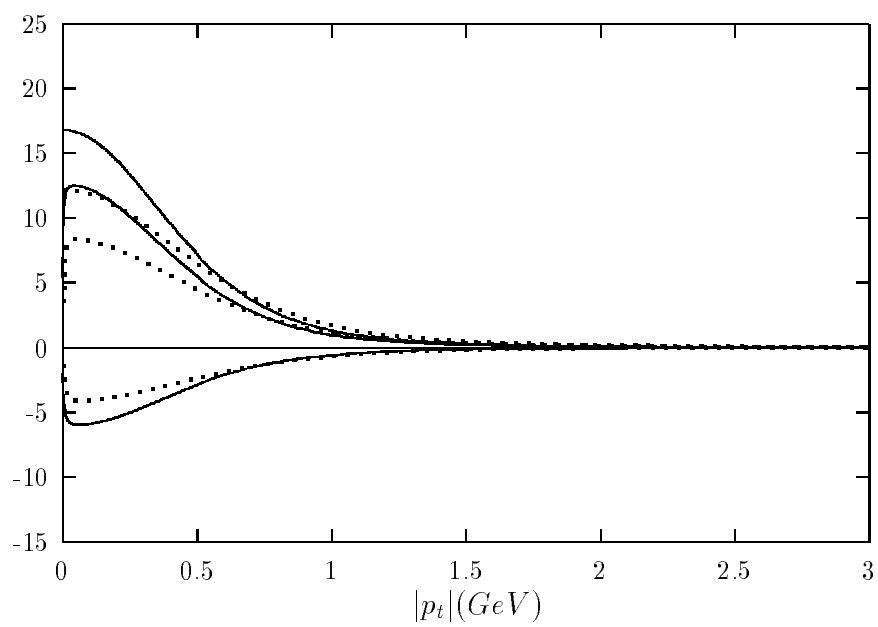


Fig.3(b)

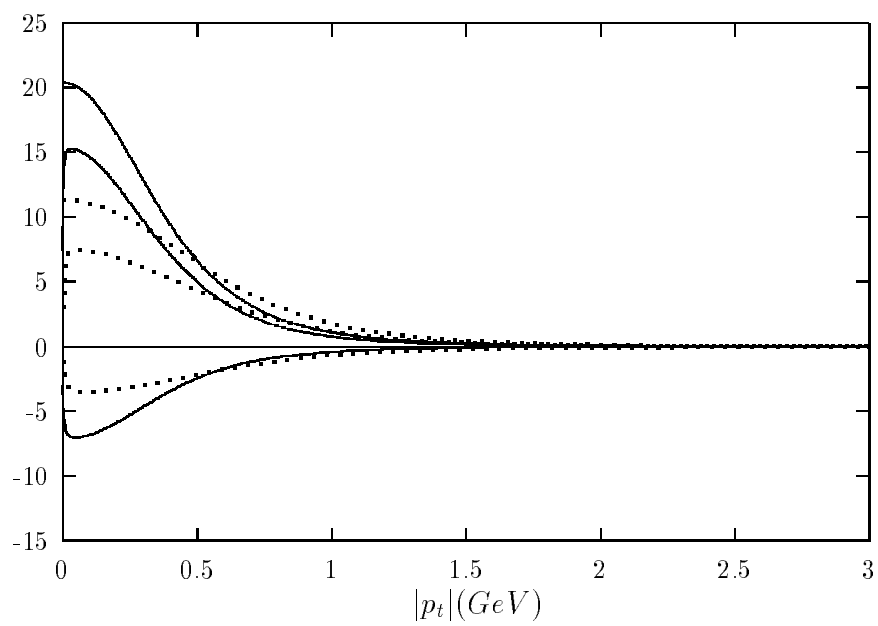


Fig.4(a)

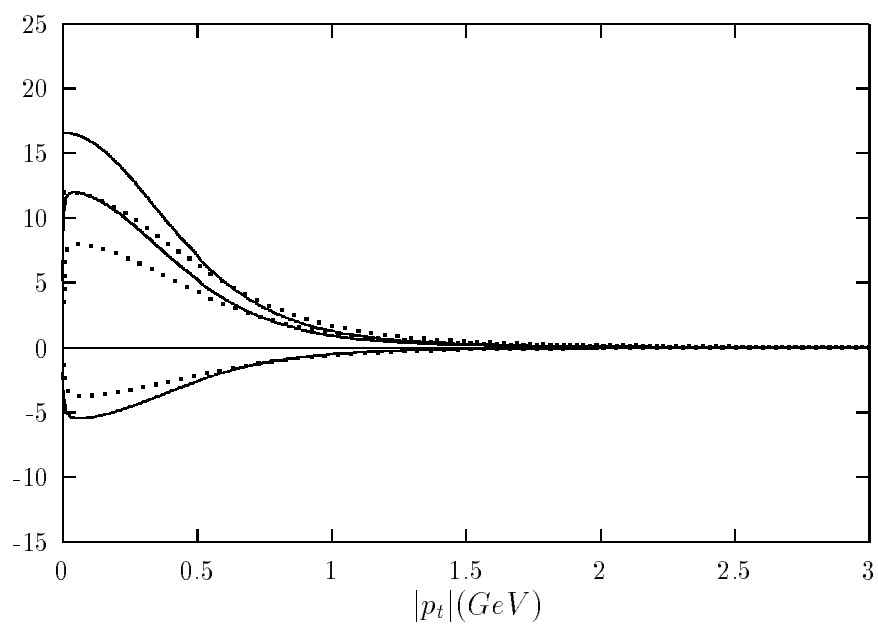


Fig.4(b)



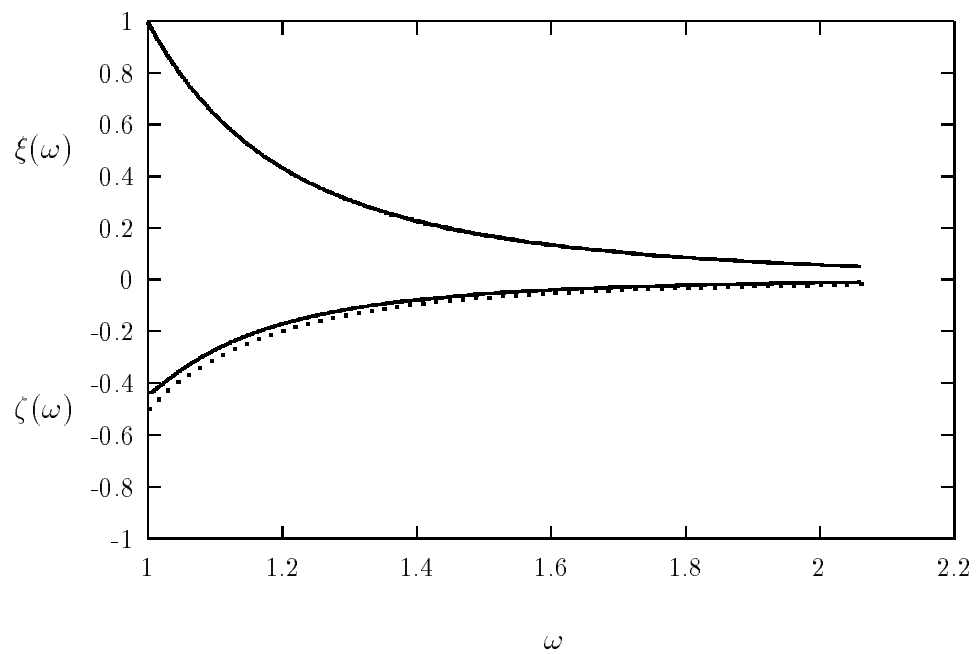


Fig.5(a)

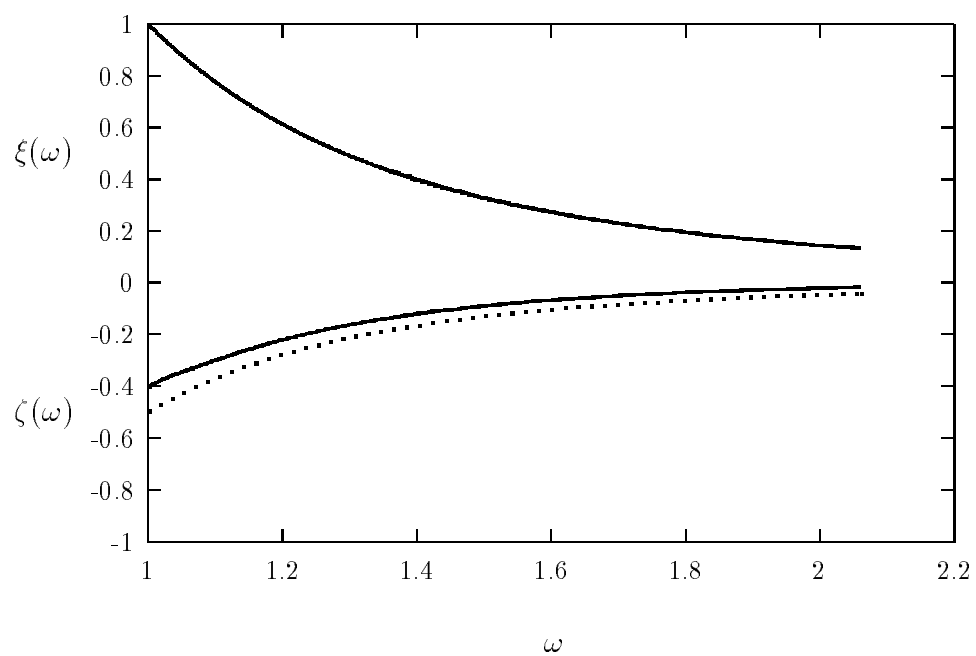


Fig.5(b)

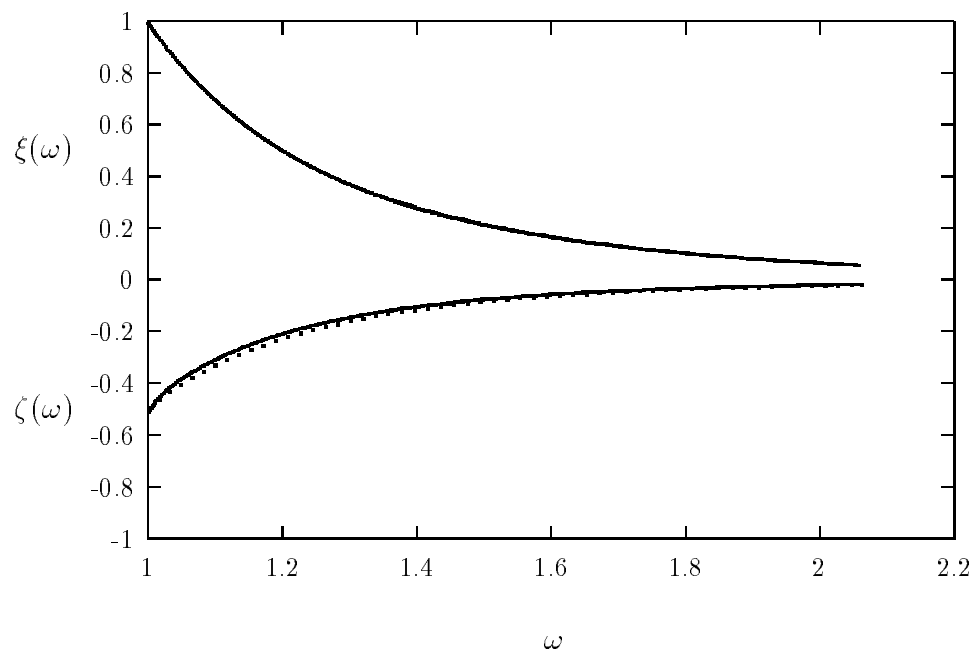


Fig.5(c)

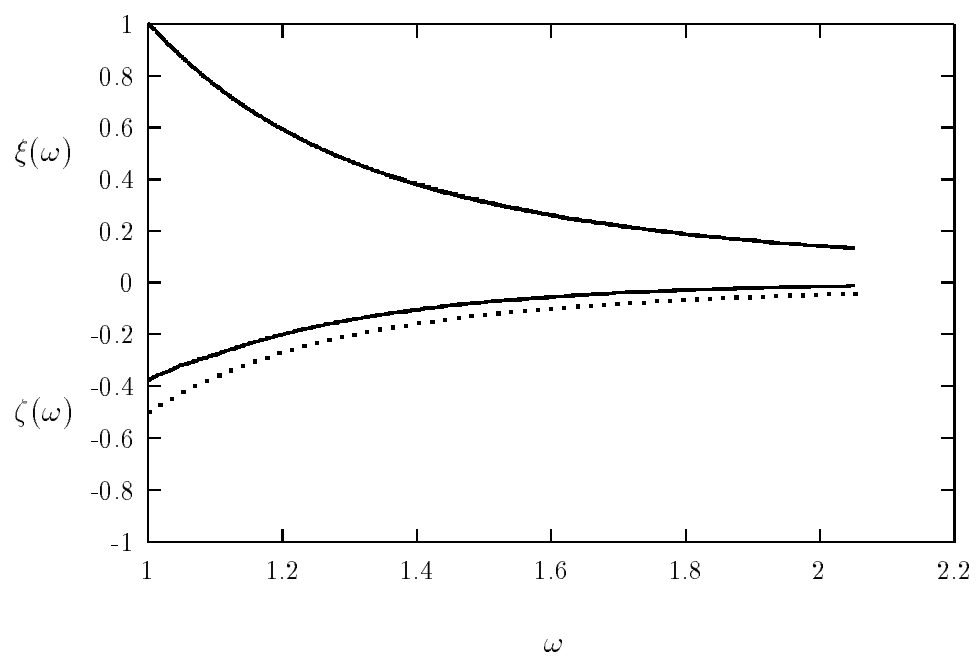


Fig.5(d)